INL/JOU-24-77041-Revision-0

Corrosion testing needs and considerations for additively manufactured materials in nuclear reactors

September 2024

Andrea M Jokisaari, Yiren Chen, Trishelle Marie Copeland-Johnson, Vineet Joshi, Isabella van Rooyen, Rongjie Song, Jonathan Wierschke, Thomas Hartmann

Changing the World's Energy Future

INL is a U.S. Department of Energy National Laboratory operated by Battelle Energy Alliance, LLC

INL/JOU-24-77041-Revision-0

Corrosion testing needs and considerations for additively manufactured materials in nuclear reactors

Andrea M Jokisaari, Yiren Chen, Trishelle Marie Copeland-Johnson, Vineet Joshi, Isabella van Rooyen, Rongjie Song, Jonathan Wierschke, Thomas Hartmann

September 2024

Idaho National Laboratory
Idaho Falls, Idaho 83415

http://www.inl.gov

Prepared for the
U.S. Department of Energy
Under DOE Idaho Operations Office
Contract DE-AC07-05ID14517

Corrosion testing needs and considerations for additively manufactured materials in nuclear reactors

Andrea M. Jokisaari[a,*], Yiren Chen[b], Trishelle Copeland-Johnson[a], Thomas Hartmann[c], Vineet Joshi[c], Isabella van Rooyen[c], Rongjie Song[a], Jonathan Wierschke[c]

[a]*Idaho National Laboratory, 1955 N Fremont Ave., Idaho Falls, ID 83415*
[b]*Argonne National Laboratory, 9700 Cass Ave., Lemont, IL 60439*
[c]*Pacific Northwest National Laboratory, 902 Battelle Blvd, Richland, WA 99354*

Abstract

Additive manufacturing (AM) technologies have developed rapidly in recent years, creating new opportunities and challenges for the nuclear industry; however, adoption requires that their corrosion performance be evaluated. We discuss known reactor-specific corrosion issues for multiple reactor types and engineering concerns such as regulations and standards. A review of corrosion studies conducted on select AM alloys informs a discussion on key bulk and surface factors likely to impact corrosion behaviors. Recommendations to assess corrosion performance for AM materials are provided, including management of the unique nature of as-built AM surfaces and the inherent process variability that occurs for AM components.

Keywords: additive manufacturing, corrosion, nuclear reactor, surface

1. Introduction

Metal additive manufacturing (AM) holds significant promise as an enabling technology for the 21st century nuclear energy industry. Metal AM can be employed to fabricate novel materials and innovative component designs unachievable through conventional manufacturing [1]. In addition, AM is poised to become a crucial enabling technology for expanding the supply chains necessary to achieve the expected increase in the number of deployed nuclear reactors [2]. Originating from rapid prototyping technology, additively manufactured components are manufactured directly from computer-aided design models, without the production of tooling. As a result of making components in a layer-by-layer fashion, AM technologies enable rapid fabrication of components with complex geometries with minimal waste. Some of the most common metals available for AM include stainless steels (SSs), nickel alloys, cobalt-chrome alloys, titanium alloys, and aluminum alloys.

Additively manufactured components can be fabricated as net-shape or near-net-shape, with the as-built surface finish being retained in the component or removed via final machining, respectively. Note that the complex geometries buildable via AM may result in both exterior and internal structures such as channels that are impossible to machine smooth or otherwise inaccessible to final surface processing. Net-shape fabrication reduces manufacturing costs by removing the final machining step; however, the surface roughness of the component is generally on the order of the size of the feedstock used for fabrication [3] and must be acceptable for the intended application of the component. A thinner layer thickness improves the surface finish but increases the building time.

The unique advantages of AM technologies have the potential to transform the nuclear industry via innovative material and manufacturing solutions for component design and supply chain [4]. The rapid development of AM technologies in recent years has already impacted many other industrial sectors [5, 6]. Successful applications of AM technologies featuring improved performance and competitiveness can be found in a wide range of engineering fields, from the automotive [7] to the aerospace [8] industries. Likewise, AM technologies also create new opportunities for the nuclear industry [9], and numerous pilot programs aimed

*Corresponding author

at employing AM technologies for current operating nuclear power plants and future advanced reactors have emerged [10, 11]. Key AM technologies deemed relevant to nuclear reactor core structures are laser powder bed fusion (LPBF), laser directed energy deposition (DED), powder metallurgy – hot isostatic pressing (HIP), electron beam welding, and cold spray [12]. These technologies are not currently in widespread use by the nuclear industry, but carry the potential to drastically reduce fabrication costs, timelines, and quality assurance burdens as well as to enable new component geometries and materials properties unachievable via conventional manufacturing [13].

Corrosion costs the existing light-water reactor (LWR) fleet in the United States approximately $4 billion a year [14]—and globally, costs are even greater. Corrosion in reactors is a vast issue that depends on the specific reactor type and the exact material system within the reactor and can occur in fuel systems and structural materials. A wide variety of reactor environments exist, ranging from high-temperature water to molten salts. Existing and proposed nuclear reactors vary widely in design, fuel type, coolant type, operating temperature, and neutron spectrum. As a result, corrosion concerns may vary significantly from one reactor to the next. This diversity of service environments poses a significant challenge to corrosion research because of the number of possible material-environment corrosion systems.

Alongside the emerging opportunities for the nuclear industry, the introduction of AM technologies poses new challenges. Evaluating the corrosion performance of components fabricated using new materials and manufacturing methods is a critical technical hurdle to their adoption into nuclear energy systems. To fully realize the benefits of AM technologies, the unique characteristics of AM materials must be understood and their impacts on in-service performance must be evaluated. In addition to layer thickness, many other variable processing parameters can influence AM component properties, including heat power, traveling speed, material feed rate, and hatch spacing [15]. Materials and components produced using AM technologies possess different defects, microstructures, and internal stress states as opposed to traditionally produced materials [1]. Consequently, the properties and service performance of AM materials can significantly differ from those of their traditionally fabricated counterparts. Little information is available on how additively manufactured materials will perform in advanced reactor environments [16, 17]. Some characteristics of additively manufactured materials, such as dislocation cells, micron-scale pores, and mesoscale compositional heterogeneity, may be critical for their performance in advanced reactor environments in which high operating temperatures, challenging chemical environments, and high neutron fluxes and fluences are anticipated.

In this work, we discuss corrosion testing needs and considerations for deploying additively manufactured materials in nuclear reactors. First, an overview of known reactor-specific corrosion issues is provided for LWRs, molten-salt reactors (MSRs), sodium-cooled fast reactors (SFRs) and lead fast reactors (LFRs), and high-temperature gas-cooled reactors (HTGRs). Next, engineering concerns related to corrosion in nuclear reactors are discussed, including the qualifications, regulations, codes, and standards regarding corrosion. A review of corrosion studies conducted on select additively manufactured metals in nuclear and non-nuclear industries informs a discussion on key factors likely to impact the corrosion behavior of additively manufactured materials, including bulk phenomena, surface phenomena, and post-build treatment. The experimental capabilities needed to perform an effective corrosion campaign for additively manufactured materials deployed in nuclear reactors are reviewed. Finally, recommendations on structuring corrosion tests for additively manufactured materials are provided, including how to manage the unique nature of as-built additively manufactured surfaces, as well as the inherent process and microstructure variability that occurs for AM components.

2. Reactor-specific Corrosion Phenomena

Corrosion issues in nuclear applications are always reactor-specific and can only be evaluated by understanding the specific alloy-environment system involved. While a wide range of materials may be used in reactor construction, the most commonly used structural materials in current reactors and future advanced reactors are nickel alloys and iron-based SSs. The corrosion behavior of a given alloy will vary depending on the service environment in which it is deployed. Because of differences in the coolant and, if present, moderator material, each reactor type has its own primary corrosion issues. Table 1 lists the typical service environments and structural materials employed for different reactor types.

Generally [18], corrosion in the context of structural alloys refers to the degradation of metallic material via chemical or electrochemical reactions with the other species of the service environment. Corrosion leads

Table 1: Service environment and structural materials for different reactor types.

Reactor Type	Environment			Materials
	Coolant	Moderator	Temperature	
LWR	Water	Water	290–320°C	Stainless steels (SS) and low-alloy steels, Ni alloys
MSR	Fluoride or chloride salt	Graphite, zirconium hydride	600–750°C	Ni alloys, SS
SFR	Sodium	-	500–550°C	SS and ferritic/martensitic (F/M) steels, Ni alloys
LFR	Lead, lead-bismuth	-	480–650°C	F/M, oxide-dispersion strengthened steels, SS, Ni alloys
HTGR	Helium	Graphite	750–950°C	Graphite, SiC, Ni alloys, refractory metals

to conversion of the metal into another species such as an oxide compound or salt. This corrosion product may remain tightly adhered to the surface of the component being corroded, may occur within the bulk of the component, or may be removed from the component surface by, for example, spalling. Passivation occurs when this reaction undergoes interference due to the presence of an adherent protective film.

For a given alloy-environment combination, various factors can contribute to the corrosion process. Table 2 summarizes the major types of corrosion that are associated with engineering alloys and may occur in nuclear reactors. While the alloy's composition and microstructure determine the general susceptibility of the material, the environment's corrosive species and pH level define the aggressiveness of the environment. The temperature at which the interactions between the material and its environment take place is perhaps the most important parameter, since it determines the rate and extent of the corrosion process [18].

Table 2: Types of corrosion associated with engineering alloys [18].

Corrosion form	**Description**	**Causes**
Uniform corrosion	Gradual, even corrosion over the entire surface exposed to the environment	Chemical and electrochemical reactions between metal and the environment
Galvanic corrosion	Electrochemical process due to the coupling of dissimilar metals in electrolyte	Formation of an anode and cathode
Crevice corrosion	Corrosion attack within narrow gaps where electrolyte is stagnant, limiting oxygen reduction, and causing differential aeration corrosion	Difference in oxygen concentration between the crevice and outside environment
Intergranular corrosion	Corrosion attack along grain boundaries, due to sensitization and depletion of protective elements	Loss of corrosion-resistant alloy elements near grain boundaries
Pitting corrosion	Localized corrosion attack in small pits or cavities, penetrating deep into the metal	Occurs in areas where the protective oxide layer breaks down
Environmentally assisted cracking	Caused by the combined action of stress and corrosive environment, classified by loading mode or cracking mechanisms	Interactions among the material, environment, and stress
Dealloying	Preferential removal of one or more alloy elements	Different dissolution rates for different alloy elements

Corrosion becomes a concern when the engineering properties of the material are degraded or the geometry of the component is changed beyond the acceptable engineering tolerances [18]. While uniform corrosion may represent the greatest loss of material in terms of quantity, it is not regarded as the most serious form of corrosion attack, as it is relatively easy to evaluate and predict. Simple tests such as immersing samples

in a fluid environment are often sufficient to evaluate the extent of uniform corrosion, and the results can be used to estimate the service lifetime of metal components. In contrast, most other forms of corrosion occur locally, and therefore the attack is limited to specific areas or parts. These forms of corrosion are more unpredictable and thus more likely to result in premature failures. Localized corrosion occurs when a small region is more susceptible to corrosion than its surroundings. Localized corrosion can include pitting, crevice, and intergranular corrosion morphologies, and frequently involves the galvanic corrosion mechanism. Localized corrosion is the larger concern for component failure, as it may cause rapid, unexpected failure.

Corrosion can interact with various other factors and mechanisms in complex ways, leading to synergistic effects that accelerate material degradation and structural failure. Irradiation can interplay with corrosion in two ways (discussed in further detail in Section 2.5): ionizing radiation can create free radicals in the coolant, increasing chemical reactivity and possibly enhancing corrosion, and irradiation can induce microstructural changes in the material that may make it more susceptible to corrosion [19]. The former effect is transient and requires ongoing irradiation to test; the latter is a persistent effect outside of a radiation field. Corrosion can also interact with creep and fatigue [18]. When the two are combined, the damage induced by corrosion can accelerate the deformation caused during creep, fatigue, and creep-fatigue. In addition, fretting can remove protective layers that prevent corrosion by mechanical wear, accelerating material loss and damage. Finally, thermal aging can lead to microstructure changes (e.g., precipitation of phases) that may make the material more susceptible to corrosion (e.g., by reducing protective elements in solution or by forming precipitates that disrupt protective films).

Corrosion protection of SSs and nickel alloys is based on the formation of a thin, adherent passive film that protects the underlying material from corrosive attack [20, 21]. These two alloy classes are widely used in nuclear reactors. There is significant overlap between the elemental compositions of nickel-based alloys and SS alloys, both having additions of Cr, Fe, and Ni. Depending on the specific grade of SS, other elements such as Mn, Mo, W, and Cu are added to improve corrosion resistance in different environments and to stabilize the fcc austenite phase. For SSs, the oxide is composed primarily of chromium oxide, whereas the oxide composition may be more complex in nickel-based alloys [18]. Although SSs, and nickel-based alloys are generally highly resistant to corrosion in many environments, corrosion may still occur [18]. In general, corrosion begins with a disruption of the oxide film, which may result from outside mechanical forces (e.g., scratching) or from localized stresses resulting in dislocations intersecting the surface. Grain boundaries can also allow secondary phases to precipitate on the surface, disrupting the film. Once the passive film has been broken, localized corrosion can begin. Ions in the surrounding medium allow for anodic reactions to corrode away unprotected regions of the alloy. This is readily seen in pitting and crevice corrosion. Localized corrosion can also occur along grain boundaries. In austenitic SSs, precipitation of chromium carbides near grain boundaries results in localized depletion of the Cr concentration at the grain boundary, which reduces the passivation and allows for intergranular attack [22]. The effectiveness of the passivation layer is also reduced by the presence of hydrogen, high concentrations of which can alter the structure and composition of the passivation layer [18]. Hydrogen also changes the electrochemical environment of the film and the base metal, reducing the stability of the passivation layer, heightening oxidation and dissolution kinetics, and promoting pitting and intergranular corrosion [18].

2.1. Light-Water Reactors

In LWRs, light water is used as both the coolant and the moderator. LWRs operate at temperatures of around 290–320°C with pressures in the range of 1000–2200 psi (6.9–15.2 MPa) [23]. The structural materials in contact with water are mostly low-alloy steels (LASs), austenitic SSs, nickel-based alloys, and zirconium alloys [19]. As a result, the main corrosion issues concerning LWRs are high-temperature aqueous corrosion of these materials. While the issues related to zirconium alloys are mostly oxidation kinetics and hydrogen pickup [24], corrosion concerns for iron- and nickel-based alloys are localized corrosion attacks exacerbated by service load and irradiation conditions in LWRs [25]. For the purpose of this paper, we focus on iron- and nickel-based structural materials, which are deployed outside of the fuel assembly itself [26].

The combination of high-temperature water and mechanical stress creates favorable conditions for stress corrosion cracking (SCC). In fact, SCC is a leading degradation mechanism for SSs and nickel-based alloys in LWRs [27]. Significant progress has been made in terms of SCC mitigation, thanks to decades of research and operational experience. Today, the water chemistry and purity is strictly controlled to eliminate corrosive species and to lower the corrosion potential [28]. Special attention has been paid to welds, where sensitization

can occur due to the thermal cycles experienced by welds [29]. Post-production heat treatment is also required to lower the detrimental effects of residual stress.

In the reactor core regions of LWRs, irradiation can not only deteriorate the material's microstructure via displacement damage, but also produce additional reactive species in the water through radiolysis. This condition leads to irradiation-assisted SCC (IASCC), a more severe form of SCC [19]. IASCC has proven a difficult issue in LWRs because many variables can simultaneously contribute to its occurrence. While irradiation defects and radiation-induced segregation (RIS) of Cr and other elements alter the material's microstructure, highly localized deformation modes also make irradiated materials more susceptible to SCC attack [30]. Despite decades of effort, a comprehensive understanding of the factors controlling IASCC has not yet emerged. In addition, flow-accelerated corrosion can affect the secondary side of steam generators in LWRs and compromise their structural integrity [31]. With flow acceleration, corrosion can take place when the protective layer on the pipes and equipment is eroded due to the mechanical effect of flow, leading to wall thinning or failures.

2.2. Molten-Salt Reactors

MSRs use liquid salts either as a coolant to remove fission heat from the fuel (unfueled salt), to entrain the fuel itself (fueled salt), or possibly both. Depending on the design, MSRs can have either a thermal or fast neutron spectrum. The salts can be either fluoride or chloride salts [32]. A mixture of salts is often selected to reduce their melting point, providing a wider operational temperature range below boiling. Unfueled fluoride salt compositions include LiF-BeF_2 (commonly called FLiBe), LiF-NaF-KF (commonly called FLiNaK), and KF-ZrF_4; unfueled chloride salts compositions include NaCl-KCl, KCl-$MgCl_2$, and NaCl-KCl-$MgCl_2$ [33]. Small quantities of other salts may be added to control the salt system's redox potential, which is a fundamental mechanism to control the corrosion behavior [34]. The nuclear fuel used in MSRs can be dissolved in molten salts, or be present in a solid form such as tri-structural isotropic (TRISO) particles [35]. MSRs are typically operated at 600–750°C, and the materials used are mostly nickel-based alloys such as Hastelloy N [34].

Molten salts are highly corrosive to most structural materials. This is due to the fact that the protective (passive) oxide films on structural materials, which are formed on the surface of materials in oxygen-containing environments such as air or water, are readily dissolved in molten salt environments and thus provide no protection against corrosion [34]. For example, alloying elements promoting the formation of protective oxide layers such as Cr and Al are prone to dissolve in molten fluoride and chloride salts [32, 36]. For this reason, Ni-based alloys are the preferred choice versus alloys with high Cr concentrations in molten salt environments.

To mitigate corrosion of structural materials, redox potential control can be employed. By introducing a reducing agent such as H_2, Be, or UF_3 and EuF_2 into the system, the redox potential can be reduced, lowering the susceptibility to corrosion in molten salts [34]. Impurities in molten salts such as moisture or tritium (from transmutation) can affect the redox potential [34]. Furthermore, in fueled salts, the fission product Te can react with Cr to form a brittle phase along grain boundaries, leading to intergranular cracking. This Te-induced embrittlement is attributed to the preferential diffusion of Te along the grain boundaries.

For a molten-salt system containing different structural materials, the local potential difference can drive the transfer of cations. In a molten-salt system, Cr removed from a component can deposit on a graphite component [37]. Similarly, if the system is not isothermal, mass transfer can occur along a temperature gradient [37]. While material dissolution occurs at the hot location, material can deposit at cold sites as a result of decreased solute solubility.

2.3. Liquid-Metal-cooled Reactors

Liquid-metal-cooled reactors fall into two classes: sodium-cooled fast reactors and lead-cooled fast reactors. Liquid metal coolants can reach higher operating temperatures than water at atmospheric or near-atmospheric pressure, improving thermal efficiency. In addition, liquid metals do not effectively moderate neutrons; fast reactors have the advantage of being effective for fissioning transuranic elements that are otherwise challenging for waste disposition.

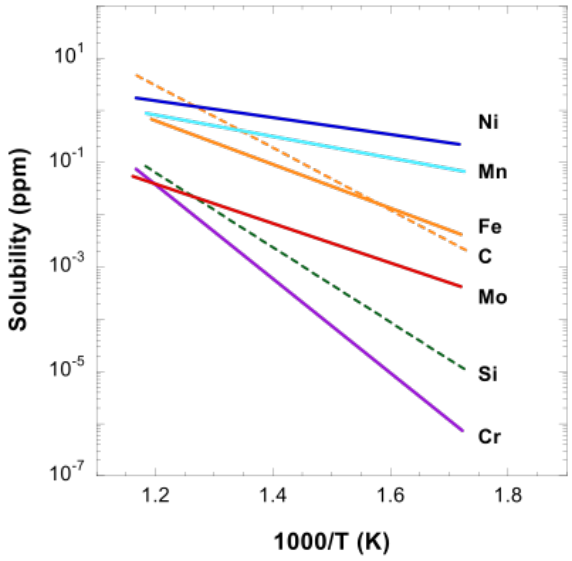

Figure 1: Solubility of alloy elements in liquid sodium (data taken from Ref. [43]).

2.3.1. Sodium-cooled fast reactors

A sodium-cooled fast reactor is an advanced reactor design that utilizes liquid sodium as a coolant and has a typical operating temperature of 500–550°C [38]. While using liquid sodium as a coolant affords significant advantages, it also poses some technical challenges. Liquid sodium reacts violently with oxygen in air to form sodium oxide, sodium peroxide, and sodium hydroxide. This reaction is highly exothermic, creating a high risk of fire with intense flame in the event of a sodium leak. In addition, liquid sodium can interact with structural materials (typically Fe-based austenitic and ferritic-martensitic [F/M] steels), leading to microstructural changes and property deteriorations [39].

Since the surface oxide layer can be readily reduced in liquid sodium, the primary corrosion concerns for a liquid sodium environment is the dissolution of the alloy's metallic elements and an exchange of non-metallic elements between the alloy and the sodium [40]. Depending on the solubility of specific elements in sodium, the alloy's constituents can be dissolved either uniformly or preferentially [39]. The surface corrosion products can be eroded or spalled into flowing sodium, giving rise to various corrosion damage types such as mass loss, surface altered layers, intergranular attack, and carburization/decarburization. Figure 1 shows the solubilities of the constituent elements of typical SSs in liquid sodium. At SFR operating temperatures, Ni is the most soluble in sodium, followed by Mn, Fe, Mo, and Cr. Due to their solubility, which is orders of magnitude higher, Ni and Mn will preferentially leach out of SSs, altering the surface composition [39]. Since Ni and Mn are austenite stabilizers, their preferential leaching will also destabilize the surface microstructure. As a result, an altered surface layer featuring the ferrite phase can be observed on the areas wetted by sodium [39]. While the effect of this selective leaching is relatively uniform near the surface, it is more evident at grain boundaries deeper in the material [41]. The depth of penetration of the surface alteration will depend on the activities of Ni or Mn in sodium.

The temperature gradient in a non-isothermal sodium system can create a condition of mass transfer through sodium flow [39]. Alloying elements selectively leached from a hot section of the sodium system can subsequently be deposited to a cold section. Similarly, if different alloys are used to construct the sodium circulation system, the difference in chemical activity can also lead to mass transfers, altering the compositions and microstructures at both the hot and cold legs. For example, the surface of a ferritic (δ phase) oxide-dispersion-strengthened (ODS) steel was found to be changed with a nickel-rich γ phase in sodium [42]. In this case, the source of Ni was from the SS components of the same loop.

Non-metallic impurities such as oxygen in sodium can react with the material, affecting the dissolution of alloying elements [39]. If liquid sodium contains sufficient oxygen, the dissolution rate of the alloy elements can become dependent on the formation energy of oxides in the sodium. At temperatures relevant to SFRs,

sodium chromate was observed to form with elevated oxygen content in sodium [44]. This reaction could increase the removal of Cr from the alloy. Nonetheless, the effect of oxygen can be successfully managed using a cold trap method. The oxygen content can be lowered substantially in the system when the cold trap is operated at < 150°C, where oxygen can be precipitated out of the liquid sodium [45].

The interactions between structural alloys and other non-metallic impurities in sodium are also of concern. Carbon is particularly important because of its critical role in SSs and its relatively high solubility in liquid sodium. Depending on the activity, carbon can be transferred from one location to another in flowing sodium [39]. In a single-material sodium system, carbon transfer manifests as a temperature-driven process, causing decarburization at the hot leg (the portion of the loop at high temperature) and carburization at the cold leg (the portion of the loop at a lower temperature). For an isothermal sodium system composed of various materials, carbon can be transferred from the high-activity material to the low-activity material. For example, in a system containing both ferritic and austenitic steels, the ferrite tends to be decarburized, while the austenite tends to be carburized [39]. The propensity of carburization or decarburization is sensitive to the carbide microstructure in the alloy. Ti- or Nb-stabilized SSs are more resistant to decarburization due to their low carbon activities, especially at high temperatures [46]. The carburization/decarburization behavior is critical to the operation of SFRs because it can directly impact the microstructural stability and mechanical properties of the structural materials.

2.3.2. Lead-cooled fast reactors

Lead-cooled fast reactors use liquid lead (Pb) or lead-bismuth (Pb-Bi) eutectic as the coolant, and operate at around 480–650°C [47]. LFR structural materials are also austenitic and F/M steels and nickel-based alloys [47]. Given the high solubilities of common steel alloying elements in Pb, mass transfers driven by activity differences will also occur in Pb or Pb-Bi systems [47]. The difference between lead- and sodium-based systems is that a stable oxide layer on the surface of structural materials cannot exist in liquid sodium, but becomes possible in liquid lead. As a result, the dominant corrosion mechanism in Pb or Pb-Bi systems is oxidation [39]. To manage corrosion, an adequate level of oxygen must be controlled in liquid lead to form a passivation layer at the LFR operating temperature [48]. Too little oxygen will be insufficient to form the protective layer, but too much will risk oxidizing the liquid Pb. Thus, the corrosion issue concerning LFRs is a balance between oxidation and dissolution. The goal is to identify the conditions (temperature and oxygen activity) that enable a passivation layer.

Another potential corrosion issue concerning Pb or Pb-Bi systems is liquid metal embrittlement. For ferritic steels exposed to heavy liquid metals, embrittlement or significant loss of ductility is observed at temperatures up to approximately 400°C [49]. Adsorption of heavy metals at crack tips or grain boundaries is hypothesized to be the mechanism that weakens the bonding along the crack path. Since the interaction between stress and corrosion contributes to the adsorption of heavy metal atoms, liquid metal embrittlement is a form of environmentally assisted cracking (EAC) in LFRs.

2.4. High-Temperature Gas-cooled Reactors

HTGRs use helium gas as a coolant and have very high outlet temperatures (i.e., exceeding 750°C) [50]. With such high operating temperatures, typical structural steels lack sufficient strength, and high-temperature nickel-based superalloys (e.g., Inconel 617), ceramics (e.g., graphite and SiC), or refractory metals must be used.

The corrosion issues concerning HTGRs arise from the impurities of helium gas. Small amounts of CO, CO_2, H_2, H_2O, CH_4, and N_2 are present in helium gas, leading to oxidation, carburization, or decarburization of structural materials [39]. Either through a gas medium or in the solid state, decarburization is a process that consumes the surface oxide layer and removes carbon from the alloy in the form of CO [39]. As a result, decarburization can lead to a carbide-denuded zone near the surface underneath the oxide layer, reducing the strength of Ni-Cr alloys [39]. On the other hand, if helium gas contains CH_4 or if the partial pressure of CO is high, the alloy can undergo a carburization process [39]. Subsequent carbide-oxide reactions can follow with the formation of Cr and CO, resulting in a porous surface scale [51]. Carbides resulting from the carburization process can also become crack initiation sites, significantly reducing the tensile strength, cracking resistance, and creep performance of nickel alloys [51].

Oxidation of Ni-Cr alloys in helium that contains impurities is controlled by Cr-H_2O and Cr-CO_2 reactions. The concentrations of H_2O and CO in helium are critical because they determine the oxygen partial

pressure and carbon activity. It is important to maintain a slightly oxidizing condition so that a Cr_2O_3 film can form, although its integrity and protective nature might be challenged at very high temperatures [52]. The presence of moisture and hydrogen in helium gas can also create conditions for decarburization, with the overall effect of the reactions between moisture and hydrogen with chromium oxide being to remove carbides while producing CO [39]. Without the gas media of moisture and hydrogen, decarburization may still occur in the solid state at the metal-oxide interface.

2.5. Corrosion Affected by Radiation

Corrosion behavior affected by radiation is a concern across all reactor types. Since neutrons and other forms of radiation (e.g., gamma rays) are inevitable in the service environment near the reactor core, radiation-affected corrosion is an issue to be addressed when evaluating the corrosion behavior of reactor materials [19]. Some topics, such as IASCC in LWRs, have been studied extensively [53], whereas others, such as those concerning the concurrent irradiation and corrosion damage in MSRs, have not yet been fully explored [54]. In general, radiation is considered a negative factor that reduces the corrosion resistance of structural materials due to the synergistic effects between radiation and corrosion systems [55]. However, in special cases, radiation can actually lead to less severe corrosion damage in structural materials [56].

The impact of radiation on corrosion arises from its interactions with both the material and the environment. By interacting with the material, radiation can dramatically change the material microstructure and microchemistry. Bombarded with energetic particles such as neutrons, protons, and alpha particles, lattice atoms in a metal can be displaced from their regular sites, leaving behind a large number of interstitials, vacancies, and defect clusters [19]. The subsequent evolution of these defects gives rise to irradiation effects such as dislocation microstructure, radiation-enhanced diffusion, and radiation-induced segregation (RIS) [19]. The resulting microstructural and microchemical changes in irradiated materials can certainly contribute to their corrosion responses. A well-known example of a radiation-affected corrosion phenomenon is Cr depletion at grain boundaries in Fe-Cr-Ni alloys [57]. RIS induces an inverse Kirkendall effect that reduces the Cr concentration while increasing the Ni concentration at the grain boundary. The decline in Cr concentration affects the passivation of grain boundaries, elevating the vulnerability to intergranular corrosion attack [19]. Similar effects can also be observed on material surfaces, where Ni and Si enrichment and Cr depletion are often detected [58]. This influence of radiation on corrosion can affect all reactor types as long as the irradiation-induced microstructure and microchemistry persist in reactor materials.

In addition to microstructural changes, radiation can also cause chemistry changes in corrosive environments. While atomic displacements may not be a concern for reactor coolants, which are either a liquid or a gas, radiation can still interact with electrons in the corrosive medium, producing radical species that can be more corrosive to alloys [55]. An example of such an effect is water radiolysis, in which water molecules are transformed into H_2, O_2, and H_2O_2 under ionizing radiation, significantly elevating the electrochemical potential of SS in water [59]. The effect of radiolysis may not be important for molten salts, since they consist of dissociated anions and cations. However, acceleration or deceleration of corrosion can occur under proton irradiation in molten salts [56, 60], suggesting a dynamic interaction between RIS and the corrosive environment. Regardless of the true mechanism(s) behind altered corrosion rates, the impact of radiation on corrosive environments is transient and will not exist without radiation during the corrosion process.

3. Engineering Concerns regarding Corrosion Behavior of Structural Components

Corrosion of structural components presents multiple engineering concerns in the context of nuclear reactors. Some specific concerns related to nuclear reactors are corrosion of the reactor pressure vessel (or any vessel in an advanced reactor design) and associated structures; and corrosion of the cooling systems, including the primary and secondary loops [61]. In terms of these concerns, first and foremost, corrosion can impact the structural integrity of components, serving as a failure mechanism that can limit their lifetimes [18]. In addition, general corrosion can release corrosion products that deposit on other parts of the plant, reducing heat transfer ability or impacting a component's mechanical ability [18]. Thus, corrosion adds to maintenance costs in terms of measuring, preventing, and mitigating corrosion in service [18]. Therefore, materials must be selected carefully, not just for their desired service properties (e.g., mechanical strength) but also for their compatibility with the service environment (e.g., to avoid pitting corrosion) and each other (e.g., to avoid galvanic corrosion).

In an engineering context, corrosion causes component failure via several major mechanisms, including loss of load-bearing capacity, embrittlement, leakage, and degradation or loss of functionality [18]. Loss of load-bearing capacity is arguably the most likely cause of component failure in a nuclear power plant. It can occur due to a relatively uniform loss of load-bearing material, such as uniform corrosion on LWR fuel cladding; the reduction of cross-sectional area; or the formation of cracks or pits throughout the material. Loss of load-bearing capacity limits the lifetime of a component as a result of inability to support the designed mechanical stresses. Embrittlement can lead to catastrophic failure of a component; components require some degree of ductility to fail via deformation without sudden, complete fracture. Leakage, which can be caused by mechanisms such as cracking or pitting, leads to the infiltration of one contained environment into another environment (e.g., coolant infiltrating past a pump seal). Degradation and loss of functionality may occur when corrosion products build up; for example, freezing a valve or clogging a heat exchanger.

In every country, the safety of nuclear power plant operations is governed by a different organization; for example, the Nuclear Regulatory Commission (NRC) in the United States, the Autorité de Sûreté Nucléaire in France, and the Nuclear Regulation Authority in Japan. While each regulator maintains authority in its own country, regulatory agencies frequently collaborate to develop best practices in a changing global landscape. The U.S. NRC is influential within the international nuclear community and plays a significant role in setting standards and guidelines for nuclear safety. Its practices are often considered by other countries when developing or updating their own regulations. Thus, the NRC considerations on corrosion and AM [12] are briefly discussed here in order to inform corrosion test plan development in the context of codes and standards.

The NRC considers corrosion a significant factor to be addressed in ensuring the safe, reliable operation of nuclear power plants. Its regulatory framework includes various requirements, guidelines, and inspections aimed at preventing, monitoring, and managing corrosion-related issues in nuclear facilities, including corrosion prevention and control. The NRC denotes corrosion allowances in several ways, such as in terms of absolute loss of thickness and acceptable corrosion rates for license applications [62]. When nuclear power plant operators apply for licensing or license renewal, licence applicants must demonstrate how they plan to manage aging effects, including corrosion, during plant operation [63]. For a material to be qualified for use in a particular application within a given plant, the environment needs to be defined and testing must show that the material can reliably perform in that environment. For critical components (e.g., reactor pressure vessels, piping, and containment structures), the NRC also requires nuclear power plant operators to select materials that are resistant to corrosion under the expected operating conditions. Beyond the initial selection of the material, the NRC mandates several monitoring systems, including environmental monitoring and in-service inspection. Environmental monitoring programs assess the quality of the cooling water, reactor coolant, and other fluids that come into contact with reactor components. This includes testing for impurities and chemical parameters that could accelerate corrosion.

Laboratory material testing for addressing regulatory needs should be informed by applicable testing standards. Before beginning a corrosion testing campaign, the needs of testing and any relevant testing standards should be identified. Evaluation of material corrosion is standardized in a series of procedures from ASTM International (formerly known as the American Society for Testing and Materials). ASTM has extensive standards for corrosion testing, and Table 3 provides a non-exhaustive list of ASTM standards potentially applicable to the testing of additively manufactured structural materials for nuclear reactors. These standards address specimen preparation, sensitization and intergranular corrosion, static and dynamic immersion tests, galvanic corrosion, pitting corrosion, SCC, electrochemical testing, and high-temperature corrosion. Some of the standards are specific to certain alloys or alloy classes, while others may be generally applicable.

Not all corrosion tests that could be envisioned for advanced reactor material-environment systems have ASTM standards. For example, no specific standards exist for high-temperature helium testing or for testing additively manufactured material. If a relevant standard does not exist, an internal standardized methodology for testing should be developed.

4. Characteristics of AM Materials Likely to Influence Their Corrosion Properties

In terms of both microstructure and surface finish, as-fabricated additively manufactured components are characteristically different from conventionally manufactured components with the same material com-

Table 3: ASTM standards applicable to corrosion testing of additively manufactured materials for nuclear reactors.

Standard Number	**Standard Name**
A262	Standard Practices for Detecting Susceptibility to Intergranular Attack in Austenitic Stainless Steels
G108	Standard Test Method for Electrochemical Reactivation (EPR) for Detecting Sensitization of AISI Type 304 and 304L Stainless Steels
G1	Standard Practice for Preparing, Cleaning, and Evaluating Corrosion Test Specimens
G31, G31/A	Standard Guide for Laboratory Immersion Corrosion Testing of Metals
G28	Standard Test Methods for Detecting Susceptibility to Intergranular Corrosion in Wrought, Nickel-Rich, Chromium-Bearing Alloys
A763	Standard Practices for Detecting Susceptibility to Intergranular Attack in Ferritic Stainless Steels
G71	Standard Guide for Conducting and Evaluating Galvanic Corrosion Tests in Electrolytes
G48	Standard Test Methods for Pitting and Crevice Corrosion Resistance of Stainless Steels and Related Alloys by Use of Ferric Chloride Solution
G46	Standard Guide for Examination and Evaluation of Pitting Corrosion
G150	Standard Test Method for Electrochemical Critical Pitting Temperature Testing of Stainless Steels and Related Alloys
G5	Standard Reference Test Method for Making Potentiodynamic Anodic Polarization Measurements
G129	Standard Practice for Slow Strain Rate Testing to Evaluate the Susceptibility of Metallic Materials to Environmentally Assisted Cracking
G59	Standard Test Method for Conducting Potentiodynamic Polarization Resistance Measurements
G61	Standard Test Method for Conducting Cyclic Potentiodynamic Polarization Measurements for Localized Corrosion Susceptibility of Iron-, Nickel-, or Cobalt-Based Alloys
G3	Standard Practice for Conventions Applicable to Electrochemical Measurements in Corrosion Testing
G102	Standard Practice for Calculation of Corrosion Rates and Related Information from Electrochemical Measurements
G82	Standard Guide for Development and Use of a Galvanic Series for Predicting Galvanic Corrosion Performance
G111	Standard Guide for Corrosion Tests in High Temperature or High Pressure Environment, or Both
G32	Standard Test Method for Cavitation Erosion Using Vibratory Apparatus

position [64], due to the very different fabrication methods employed. While additively and traditionally manufactured materials can be compositionally similar, their corrosion behaviors may differ, as both AM microstructures and the AM surface finish may play a critical role in corrosion. Due to the high cooling rate and rapid solidification commonly associated with AM technologies, additively manufactured materials often exhibit dendritic microstructures and high-temperature phases that significantly impact their corrosion resistance [65]. Characteristics of additively manufactured materials, including surface roughness, dislocation cells, porosity, and compositional heterogeneity [3, 66], raise concerns over their corrosion performance in advanced reactor environments. In addition, post-build heat treatments alter the AM microstructure, giving rise to a wide range of secondary phases or precipitates, which could also have significant consequences on the corrosion behavior of the material. Furthermore, in-service evolution of AM microstructures, such as that caused by thermal exposure or irradiation damage, can complicate the situation even further by introducing new interaction mechanisms or affecting the existing interactions to a different extent. To provide specific examples, the following discussion focuses on the behaviors of 316 SS due to its overall utility throughout the nuclear industry [4].

As AM has increased in engineering feasibility, corrosion testing of AM materials has followed. However, the variety of AM techniques and the complexity of AM microstructures that can occur in a given composition of material (e.g., 316 SS) mean that a clear picture has yet to emerge on the exact interplay between manufacturing parameters (resulting in microstructure) and corrosion behavior. Although surface roughness is known to impact corrosion properties [67], most AM corrosion studies have been conducted on milled and polished samples [67]. Some studies on polished specimens indicate that the corrosion resistance of additively manufactured SSs is improved versus their conventionally wrought counterparts when exposed to water and sodium chloride environments [68] despite the complexity of the interplay between microstructure and corrosion mechanisms, and provided that the material does not contain significant porosity. Increasing both porosity and pore size increases the SCC growth rate [69]. There is also evidence that increasing porosity decreases the breakdown voltage of SSs [70]. Furthermore, if the solidification microstructure contains δ-ferrite, this microstructural inhomogeneity could also alter the corrosion response [71]. As shown in numerous studies [72–74], the inhomogeneous microstructure resulting from the solidification process can impact the corrosion behavior of additively manufactured materials. As a result, this AM-specific corrosion issue must be characterized and understood.

Conversely, much remains to be explored regarding the effect of surface roughness or surface features on the corrosion of additively manufactured 316 SS material and the corrosion of additively manufactured components for nuclear applications. Several studies examined the effect of surface modifications on corrosion behavior (e.g., sandblasting), as well as the effect of build surface orientation on corrosion [3, 70, 75]. Mixed results were seen for surface modifications intended to smooth the component, with some modifications improving the corrosion behavior and others making it worse [67]. Build surface orientation had a clearer impact, although other factors impacting the microstructure, rather than just the surface roughness, could also be responsible [67]. Regarding the actual surface features, it was found that surface slags, that is, Mn-rich silicate oxide particles, promoted pitting corrosion of 316L fabricated by LPBF in a sodium chloride water solution [76]. These slags introduce cracks and other heterogeneities in the protective oxide film on the surface. Finally, very little work has been published to date regarding the corrosion of additively manufactured components for nuclear applications, and the focus has been on water environments [69, 77–79]. However, the information on additively manufactured material corrosion in water and sodium chloride environments should be transferable (within limits) to the corrosion behavior of additively manufactured materials for nuclear applications, especially in the context of other corrosive environments such as liquid metals, molten salts, and high-temperature helium, provided a mechanistic understanding of corrosion and microstructure is applied.

4.1. Bulk Phenomena

Laser-based AM techniques such as LPBF produce heterogeneous and anisotropic microstructures as a result of the layer-by-layer nature of the manufacturing process coupled with rapid solidification and large spatial thermal gradients [80]. In LPBF 316L, the intrinsic multiscale chemical heterogeneities (e.g., solute segregation, Cr depletion, and precipitate formation) inevitably alter corrosion performance. Galvanic corrosion, pitting corrosion, dealloying, carburization/decarburization, and intergranular corrosion and cracking are all phenomena potentially affected by AM microstructure and microchemical heterogeneities.

4.1.1. Residual stress

Residual stresses from the build process can be significant enough to cause visible warping of as-built components upon their release from a build plate [80]. Laser-based AM processes can result in very high thermal gradients locally; combined with rapid cooling and repeated heating from layer-by-layer building, residual stresses can be significant in as-built AM components [80]. These stresses tend to be compressive inside AM components and tensile on the component surface [81]. Residual stresses are often highest along the build direction. In addition to causing geometrical problems such as distortion or delamination, residual stresses are known to impact passivity [70] and EAC susceptibility [82], especially when the stresses are in tension and exceed the yield stress. SCC in additively manufactured 316 SS followed the build direction of stress-relieved 316L SS built via LPBF, while recrystallized material had a similar SCC growth rate as wrought material [69].

Due to the critical role of residual stresses in the performance of additively manufactured materials, process strategies such as scan pattern and temperature control can be employed to help manage residual stresses [80]. More importantly, post-build heat treatment is frequently necessary to relieve residual stresses and mitigate the impact on corrosion performance [80]. While residual stresses may not be a problem unique to additively manufactured materials, they can significantly impact corrosion performance. Thus, particular attention must be paid to managing residual stresses and minimizing their impact on the corrosion resistance of additively manufactured materials.

4.1.2. Porosity

Build porosity is also a concern, with pore volume fractions of 5% or more being possible (depending on the processing parameters) [83], although full density is typically targeted. As a matter of course, additively manufactured materials contain defects such as microscale pores or larger lack-of-fusion cavities [80]. While both types of defects are empty voids within an otherwise sound solid, they show distinct morphologies (e.g., irregular, ellipsoidal, or spherical) and have different origins (e.g., from trapped gas or partially melted powder) [80]. The overall quantity of these defects can be measured by the porosity level. AM processing parameters such as the energy density of the laser beam and the feedstock properties can considerably influence the porosity level [80]. Mechanically, pores and cavities are stress risers, which can facilitate crack initiation. Chemically speaking, they are sites vulnerable to pitting or other forms of localized corrosion if a corrosive medium is present. Lack-of-fusion cavities can provide crevice-like occluded areas that promote the development of aggressive corrosion chemistry [84]. The effect of porosity on SCC susceptibility remains unclear at present. While one study on cold-worked additively manufactured materials seems to show a positive correlation between porosity and SCC susceptibility [69], another study involving as-printed materials containing low porosity did not show any effect of porosity on SCC [85]. Regardless, porosity is a characteristic of additively manufactured materials, and its influence on corrosion should be treated as an AM-specific corrosion issue.

The metastable pitting characteristics of AM LPBF-built 316L SS with different porosities were compared against wrought 316L SS by using potentiostatic testing [86]. The number of metastable pitting events were normalized to surface area and exposure time in order to obtain a pit formation frequency. In addition, the pitting potential and corrosion potential were measured. A pitting potential is defined as the potential at which the protective passive coating breaks down and the characteristic of the electrochemical system becomes transpassive. The test results showed that the porosity of additively manufactured LPBF 316L SS does affect the metastable pit formation frequency, though the measurement of the pitting potentials of LPBF 316L SS shows large standard deviations. However, as an overall trend, the pitting potential of LPBF 316L SS is an improvement over that of wrought 316L SS, even at the highest pit formation rate. Conversely, the corrosion potentials do not show any noticeable differences. LPBF 316L SS shows a significantly higher pitting potential than that of the wrought 316L SS, but a very similar corrosion potential. The corrosion potential did not reflect a clear trend with porosity, and the corrosion current densities of the LPBF samples were somewhat higher than those of their wrought counterparts.

4.1.3. Heterogeneous and anisotropic microstructures

The microstructure of additively manufactured materials is generally complex. Unlike traditionally manufactured materials, additively manufactured materials have a complex solidification microstructure [80]. The details depend on the material and process involved, but melt pool boundaries are generally visible

at the macroscale in fusion-based methods, and individual grains (defined by high-angle grain boundaries) are generally elongated along the thermal gradient present during the build process. Within each grain, a cellular dislocation structure generally occurs during AM builds of SSs and other metals [16] (similar to the dislocation cell structure that occurs during plastic deformation), and may also have solute segregation to the cell walls. Additionally, other phases may be present in additively manufactured material but absent in conventional material of the same composition [80]. Oxide phases or atypical inclusions may be present in additively manufactured materials as a result of feedstock oxidation or other contamination, while previously unreported phases may occur due to the rapid cooling and repeated thermal cycling in AM build processes. The presence of these phases can affect the stability or quality of a protective oxide film, altering the corrosion behavior in comparison to that of a wrought analog [80]. The presence of δ-ferrite may alter the corrosion of additively manufactured 316 SS, likely due to its impact on the formation of the chromium oxide passive film. The presence of δ-ferrite within 316L SS fabricated by powder DED affected its IASCC behavior compared to that observed in wrought material [77]. Cracks propagated along the δ-ferrite/γ-austenite phase boundaries, likely because of the reduction in grain boundary sliding and because of dislocation interactions at boundaries providing crack nucleation sites [77]. Anisotropy of the δ-ferrite distribution in 316L SS fabricated via wire arc AM also affects pitting and uniform corrosion rates, with less phase volume and more finely dispersed δ-ferrite, thus improving the general corrosion rate [87]. The σ phase is also detrimental and has been reported to increase pitting corrosion [88]. Heat treatment generally improves corrosion behavior [89], likely due to the dissolution of deleterious phases.

Related to the solidification process, additively manufactured materials often exhibit columnar or irregular grain structures or textures [84]. Grain growth following the solidification of the melt pool tends to be along a certain crystallographic orientation. The resulting texture depends on the thermal gradient and the solidification rate, and can thus be controlled by process parameters. Scan strategies that give rise to more homogeneous melting and solidification reduce the degree of printing texture [84]. The presence of an anisotropic grain structure can influence corrosion properties such as pitting, localized corrosion [81], and SCC susceptibility [69]. While the issue of anisotropic grains is certainly not unique to additively manufactured materials, it is a specific issue to be addressed when corrosion performance is of concern. Several studies have demonstrated that process control can minimize the detrimental effects of anisotropic grain structure on the corrosion performance of additively manufactured materials [68, 69].

The microstructure and corrosion resistance of 316L SS samples prepared using LPBF and DED were compared with those of wrought material [68]. During fabrication, LPBF created smaller melt pools and produced much finer cellular microstructures than DED, and this was found to affect the corrosion properties of additively manufactured 316L SS. The mean grain size of wrought 316L SS is about 20–30 μm coarser than the cell sizes in the microstructures of DED 316L SS and LPBF 316L SS (about 4 and 0.7 μm, respectively). Different manufacturing conditions produced materials of different microstructures—but fairly similar corrosion potentials and passive current density values, though the passivation potential was strongly impacted. The passivation potentials of the materials, however, showed variations in the following order: LPBF material > DED material > wrought material. These results imply that with finer microstructures, the passivation surface layer of SS is maintained at far higher potentials until the passivation layer breaks down and the system becomes transpassive. Therefore, additively manufactured LPBF 316L SS showed the highest (most noble) passivation potential associated with its finer microstructure, which is thought to lead to a more stable protective oxide layer [68].

Intergranular and intragranular Si- and Mn-rich oxide inclusions are present in laser additively manufactured austenitic SS [90]. Alloying elements such as manganese, molybdenum, and silicon have a strong affinity to oxygen and will form oxide particles. Silicon-rich oxide inclusions in additively manufactured 316L SS will reduce impact toughness and SCC properties [91]. The intragranular oxide inclusions promote early microvoid formation, reducing the impact toughness relative to wrought materials and materials fabricated using powder metallurgy – HIP (all of comparable grain sizes) [92]. A higher volume fraction of oxide inclusions is expected to reduce the impact toughness and increase the SCC susceptibility of additively manufactured materials in high-temperature water [92].

The higher oxygen concentrations of additively manufactured materials, relative to wrought alloys, are a result of adsorbed oxygen in the alloy feedstock powder [90]. During manufacturing, micrometer-sized oxides with Mn, Mo, or Si form. The uniform oxide dispersions in additively manufactured materials may disrupt the continuity of the passivating film, impacting its corrosion behavior [93]. The control of oxygen and high-

oxygen-affinity elements such as Si during additive manufacturing may help reduce oxide formation. Further studies are needed to enhance our understanding of process-related oxide formation. AM powder feedstock should undergo rigorous quality control to ensure as low an oxygen surface concentration as possible, and suitable protocols must therefore be established.

4.1.4. Cellular substructure and segregation

For the composition of 316 SS, dendritic growth prevails during solidification, giving rise to solute segregation (e.g., Ni, Cr) and a dislocation cell structure [94]. This cellular substructure is on the order of 1 μm in size, though this varies depending on the build parameters [94]. The dislocation cell structure consists of cell walls on the order of tens of nanometers thick, composed of tangled dislocations and relatively dislocation-free cell interiors. The dislocation cells may be either equiaxed in all three dimensions, or columnar in nature with the small dimensions being approximately equal [94]. The cellular microstructure of additively manufactured 316L has a non-equilibrium nature and shows enrichments of mostly all alloying constituents—Cr, Ni, Mo, Mn, and Si—at the microstructure cell wall, while the cell center, as a result of incomplete solutionizing, is enriched with iron.

This unique heterogeneous microstructure can have important implications on corrosion behavior. In a biological environment, a dislocation cell structure was found to improve the passivating behavior by providing a high density of oxide nucleation sites [72]. The dislocation cell walls could also promote the growth of denser, more stable passive film [68]. However, the results are mixed, and defects can become a dominant factor for the corrosion response [73]. Galvanic coupling may occur between the iron-rich cell center and the more noble cell wall. Solute-depleted cell interiors could undergo preferential attack in oxidizing environments, with the iron acting as a sacrificial anode, electrochemically protecting the more noble cell wall with relative higher concentrations of Cr, Ni, Mo, Mn, and Si. Without solution annealing, the corrosion of iron in additively manufactured 316L SS would therefore be enhanced. Since the heterogeneous microstructure originates from solidification, AM process parameters influencing the heating and cooling of the melt pool and overall build are important. For example, the extent of solute segregation can be controlled by altering the scan speed [74].

AM process parameters are important in regard to the corrosion performance of additively manufactured materials. Specimens of additively manufactured LPBF 316L SS were produced at print speeds of 550, 650, and 700 mm s^{-1}, and their corrosion potentials and corrosion current densities were then measured [95]. With increasing print speed, dislocation structures become more pronounced. Increasing the printing speed from 550 to 700 mm s^{-1} promotes finer microstructures, decreases the average lattice parameter, and increases dislocation densities. Higher printing speeds promote enhanced solidification rates within a single print track, affecting the solidification microstructure. Consistently, the largest lattice contraction and dislocation density was reported for the specimens printed at 700 mm s^{-1} [95]. The reduction in lattice parameter is driven by dealloying and Cr depletion from the austenite matrix phase, resulting in Cr segregation to the boundaries of the cellular microstructures. The increased dislocation density induces some changes in corrosion potentials as measured using cyclic voltammetry. Samples printed at higher speeds show larger hysteresis eventually derived from disruption of the passive oxide film layer with subsequent stable pit growth, and hence an elevated anodic current, until repassivation conditions are reached [95]. Corrosion and pitting potentials move slightly to the more noble region, but the data scattering is too large to formulate a solid quantitative statement about how the dislocation structure impacts electrochemical potentials.

Faster scan speeds and a more pronounced dislocation structure can, in comparison to wrought counterparts, lower the pitting potential and increase the susceptibility to pitting corrosion, but reverse effects are also possible [95]. Overall, the data scattering is large. The repassivation potentials of LPBF 316L SS produced at low printing speeds are lower than those of wrought 316L SS, while at high printing speeds and high defect densities, the data scattering is too large for quantitative statements. It seems obvious that the reproducibility of dislocation structure at high scan speeds is low and the data scattering is therefore high, diminishing the quality of any trend quantifications.

For now, it is fair to state that increasing the dislocation densities produces lower (less noble) corrosion potentials and lower passivation current densities in LPBF 316L SS. Wrought 316L SS shows corrosion potentials similar to those of the specimens produced at 650 mm s^{-1}, combined with low passivation current densities such as those seen in the 700 mm s^{-1} specimens. In the AM fabrication process, a low print speed enables more noble corrosion potentials but far larger passivation current densities.

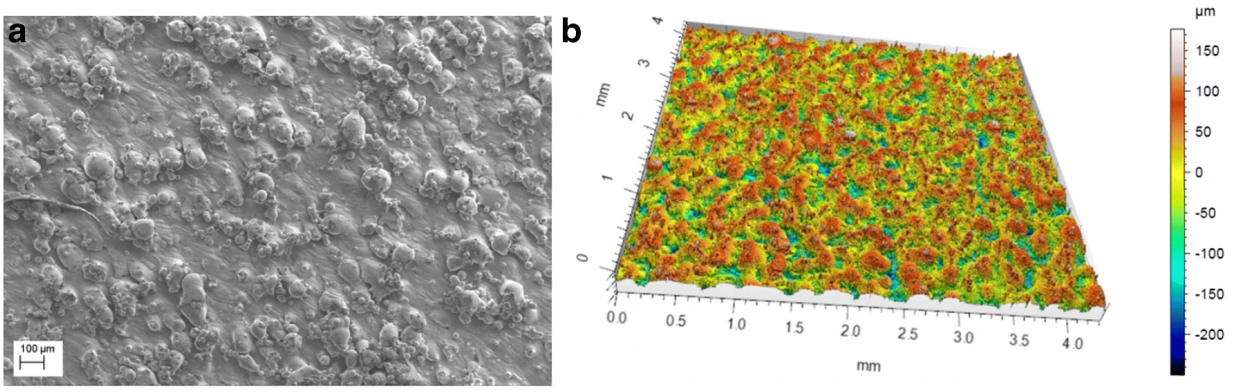

Figure 2: Surface roughness of LPBF-built samples of a copper-chromium-zirconium alloy. a) Unmelted powder particles on the surface. b) Surface profile of the surface in (a) with an average surface roughness of 40 μm $\pm$5 μm. This image is reproduced from Ref. [99] with cropping of two additional subfigures under the Creative Commons Attribution 4.0 International License [100].

4.2. Surface Phenomena

The corrosion behavior of additively manufactured components depends on the surface finish. While traditionally fabricated components generally have a machined surface, one benefit of AM processing is the building of net- or near-net-shape components. Without post-build surface machining, surface roughness resulting from the AM process is a macroscopic concern. The surfaces of additively manufactured components typically have a roughness on the order of the feed powder or metal wire used during the build [**?**]. For example, the surface roughness for components produced via LPBF is on the order of microns and generally ranges from 10 to 30 μm [3], and is about one order in magnitude higher than the surface roughness of parts produced via conventional manufacturing techniques such as milling (0.8 μm), honing (0.1 μm), or lapping (0.05 μm). Figure 2 illustrates the surface roughness of a LPBF-built specimen, including the presence of unmelted powder particles. The surface roughness of wire DED specimens is on the order of 1 to 8 μm, and that of powder DED specimens is on the order of 3 to 43 μm [96]. Wire DED may also produce components with macroscopic layers visible to the eye, sometimes termed ripples [97] (Fig. 3), which are not captured in surface roughness measurements, but which should be considered for corrosion. In all of these cases, this roughness may be sufficient to promote localized crevice corrosion. Another concern is porosity intersecting the surface (or just under the surface, to be revealed after some amount of uniform corrosion), and this is another source of possible crevice corrosion initiation. In addition, AM surface features such as balling (droplets), staircasing (surface curvature), and partially fused powder particles can result in crevice-like defects [80]. Formation of surface defects depends on the angle and orientation of the printed piece during printing, and some surfaces are rougher than others [98]. Surface roughness is also affected by printing parameters such as the energy density of the energy source and the hatch distance [98]. Surface remelting can reduce roughness on the top surfaces, but may not help the inclined surfaces [98].

The effect of surface roughness on the corrosion behavior of 316L SS manufactured via LPBF was studied by surface grinding samples to reduce the surface roughness from 2.8 ± 0.6 μm to 0.07 ± 0.04 μm [75]. Three different corrosion environments were used: 3.5 wt% NaCl water solution, 3 wt% H_2SO_4 solution, and high-temperature oxidation at 800°C. Decreasing the surface roughness of additively manufactured LPBF 316L significantly impacted the material's electrochemical behavior and thus its corrosion properties. Reducing the surface roughness decreased the corrosion current densities and shifted the corrosion potential in the positive (more noble) direction. The surface-treated specimens, because of improved passivation layers, showed higher corrosion resistance, while in electrochemical tests the as-built LPBF 316L SS with the rough surface showed less corrosion resistance. In high-temperature oxidation experiments, the lowest mass gain was found in the surface-treated specimens [75]. Overall, surface finish is a key contributor to the corrosion performance of additively manufactured materials and should be carefully characterized and managed to ensure adequate corrosion resistance in the relevant service environment.

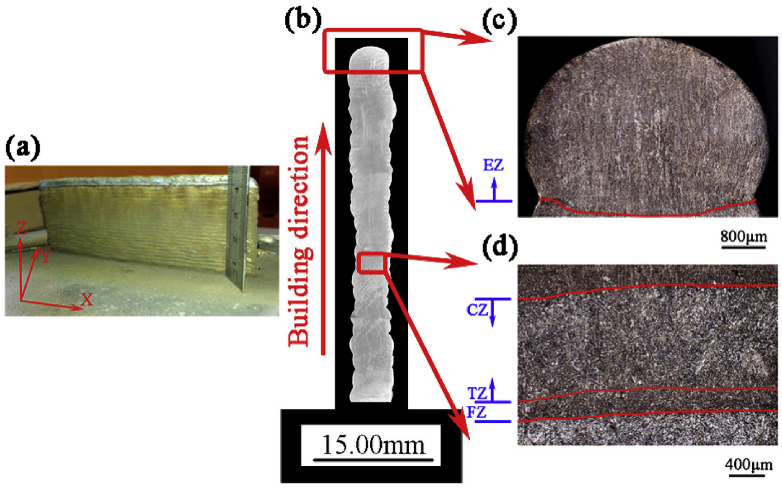

Figure 3: As-fabricated thin-walled specimen built by wire arc additive manufacturing (wire DED). a) Macroscopic component showing ripples between deposition layers, b) cross section of the thin-walled specimen, c) and d) grain structure in different portions of the build. Reproduced with permission from Ref. [101].

4.3. Post-build Treatments and Process Variability

Given the features of additively manufactured materials (e.g., surface roughness, solute segregation, complex microstructure, and residual stresses), some amount of post-build processing generally occurs [80]. The surface may be machined, as previously discussed. Post-build heat treatment is also common for stress relief, solution annealing, or microstructure homogenization [7]. However, post-build processing incurs additional time and cost; generally will not resolve the presence of additional oxide phases, atypical inclusions, and build porosity; and may or may not remove the original build microstructure.

The impact of the unique microstructural features of additively manufactured 316L SS on corrosion fatigue behavior was studied for high-temperature water under boiling-water reactor (BWR) and pressurized-water reactor (PWR)-type oxidizing conditions [69]. Additively manufactured LPBF 316L SS was heat treated to produce variations in microstructure and residual plastic strain. Three different heat treatment conditions were used to assess the effects of microstructure variations on corrosion fatigue crack growth behavior: (1) stress relief at 650°C for 2 hours in argon, (2) HIP for 4 hours at 1150°C and 100 MPa in argon, and (3) heat treatment at 955°C for 4 hours in argon. After appropriate heat treatment, LPBF 316L SS can exhibit a corrosion fatigue crack growth response in high-temperature water, similar to that of its wrought counterpart [69]. However, HIP treatment did not lead to significant improvement over the stress-relieved condition in terms of porosity. Solution annealing (955°C for 4 hours) was selected in order to produce a bimodal microstructure involving both recrystallized equiaxed grain and as-built characteristics. However, full recrystallization was not always achieved, due to the strain variations at different locations of the as-built part, and some un-recrystallized grains remained [69].

Cold-worked SSs are known to be susceptible to corrosion fatigue and SCC in the high-temperature water typical for BWR or PWR conditions. The as-built material, cold-worked in different directions, resulted in different crack growth rates. Stress-relieved additively manufactured 316L SS exhibited a far higher crack propagation rate along the build direction than normal to the build direction. Stress-relieved additively manufactured 316L SS cold-worked along the build direction resulted in crack propagation rates similar to those of cold-worked additively manufactured 316L SS that had undergone HIP and solution annealing. This orientation dependency in stress-relieved material is explained by its anisotropic microstructure [69]. Wrought 316L SS showed lower corrosion fatigue rates than additively manufactured LPBF SS after being stress relieved and undergoing HIP and solution annealing. Especially at low-load frequencies, the crack growth rates of stress-relieved additively manufactured LPBF 316L SS are more than double those measured in wrought 316L SS.

The impact of process variability on the properties of additively manufactured materials is a significant concern that extends to their corrosion behavior. In this context, process variability refers to variations in the as-built microstructure from a single, specific machine. Even with the same build parameters being

used in the same AM machine (e.g., laser power, scan pattern, and speed for LPBF), sources of process variability include, but are not limited to, the laser power and scan speed [80]; feedstock lots; atmospheric storage condition of the feedstock, especially powder feedstock; atmospheric composition during the build, including humidity levels [102]; and heat dissipation during the build as a result of build plate heating, the surrounding atmosphere, and the build geometry [80].

The geometry of the as-built specimen from which corrosion samples are removed should be considered a part of process variability. It is conceivable to take corrosion specimens from short builds with limited build volume, even though the actual component will be larger. Given the impact of build volume on thermal history and the resulting microstructure, corrosion specimens sectioned from builds whose geometries and volumes are representative of the actual component may also need to be assessed.

5. Experimental Capabilities Required for Corrosion Research on Additively Manufactured Alloys

To characterize the corrosion behavior of materials, various test methods may be used to evaluate the extent of a corrosive attack. These tests can be as simple as measuring the changes in the sample's weight and thickness after exposure to a corrosive environment, or as complex as *in situ* monitoring of crack development under simultaneous corrosion attack and thermomechanical degradation. To understand the corrosion mechanisms of additively manufactured materials for nuclear reactor applications, the tests may be focused on engineering quantities such as macroscopic weight loss/gain or mesoscale features such as local compositional changes. Regardless of the complexity of the experimental methods, the purpose of corrosion testing is to reveal the nature of the corrosive attack and to quantify the extent of material deterioration in a specific corrosive environment.

Corrosion test methods can be broadly categorized into three types: immersion (including static and flowing fluid, both liquids and gasses), electrochemical, and mechanically assisted or irradiation-assisted tests [18]. For laboratory corrosion tests, the samples are usually small and their surface conditions can be effectively controlled. The corrosive environments relevant to nuclear applications include water, liquid metals, molten salts, and helium with impurities. Since elevated temperatures and pressures are present in reactors, autoclaves are often needed to simulate reactor service environments.

5.1. Immersion Tests

Static immersion tests are generally executed in capsules and provide a measure of general corrosion behavior. They are a good screening method for eliminating materials incompatible with the test environment. Small coupon specimens prepared from the materials of interest are exposed to the test environment, and the specimens' weight and thickness changes are measured as a function of exposure time [18]. Weight measurements are used to determine the weight loss or gain of the sample, indicating either the removal or addition of material (often oxide formation). Thickness measurements provide similar information about material loss/gain. In addition to weight and thickness measurements, other characterization techniques can be used for post-exposure examination of immersed samples. Optical and electron microscopy can provide information on the surface morphology and the nature of the surface layer, which is valuable to understand the underlying corrosion mechanisms. In addition, immersion tests can also be performed with stressed samples. Static loading can be readily implemented in immersion tests with U-bent or C-ring specimens [103], simulating the corrosion conditions favorable for SCC initiation.

Flowing immersion tests are typically executed as loops. These tests simulate real-world scenarios in which materials are exposed to corrosive environments while the fluid is flowing (e.g., coolant flowing through pipes or heat exchangers) [41]. The fluid flow rate can be adjusted to simulate specific operating conditions. One major difference between static tests and flowing tests is that the corrosion rate in static tests will decrease as corrosion progresses, due to saturation of species in the fluid. However, loop tests with a hot leg (the portion of the loop containing the sample) and a cold leg (the portion of the loop without the sample and at a lower temperature) will typically result in deposition of the species in solution at the cold leg due to increased solubility, ensuring the corrosion process continues at a high rate.

Both static and flowing tests are sensitive to the choice of capsule and loop material. The capsule and loop material should be inert with respect to the corrosive environment and should also be compatible with the sample material. For example, the capsule material should have negligible solubility for elements within

the sample material; otherwise, an inadvertent corrosion cell could be created. In addition to capsule and loop tests, exposure to gases or vapors can be considered as immersion tests. These tests may also be executed in static or flowing conditions [18].

5.2. Electrochemical Tests

Electrochemical tests are focused on control and measurement of the fundamentals of electrochemical reactions and are used to assess a material's corrosion resistance and passivation properties [18]. Using the electrical current, potential, and resistance properties of the electrochemical cell, these tests can provide insights into how materials respond to oxidation and reduction processes. The electrochemical potential is a good measure of the driving force of the reactions that occur at the anode and cathode, and the current density is an excellent representation of the rate of the reaction. Based on the principle of the electrochemical cell, several types of electrochemical tests can be developed, including potential, resistance, current, and polarization measurements [103]. These tests can be used to determine the galvanic series, level of cathodic protection, corrosion rate, susceptibility to pitting, etc. These fundamental corrosion properties can then be used to aid in the development of corrosion-control strategies and implementations.

5.3. Assisted Corrosion Tests

Mechanically assisted corrosion tests are particularly important for approximating the conditions encountered in service, since they emulate the simultaneous presence of mechanical loading and a corrosive medium [18]. While immersion and electrochemical tests can adequately emulate a well-defined material-environment system, mechanical damage that may influence corrosion deterioration is not evaluated. Apart from certain limited cases, the effects of mechanical loading on the development of corrosion degradation is not considered in immersion or electrochemical tests. In real-world applications, however, the synergistic effects arising from the interaction between corrosion and mechanical degradation are often the controlling factors for the most dangerous forms of corrosion attack, such as SCC or corrosion fatigue. Mechanically assisted corrosion tests are designed to closely represent these types of service conditions and to measure the material properties directly related to the failure mode. For example, if cracking is the expected failure mode, fracture mechanics properties such as crack growth rate or fracture toughness are measured. Although these tests are more complex experimentally, the information they can provide is highly relevant to the service performance.

Irradiation-assisted corrosion tests aim to explore the synergy between two damage mechanisms: radiation and corrosion. As discussed in Section 2.5, radiation exerts its influence on corrosion, both by modifying the material microstructure and changing the chemistry of the environment. When the effects of radiation-induced microstructure evolution are of interest, material irradiation and corrosion testing can be performed sequentially, as the irradiated microstructure persists beyond the end of the irradiation. From a technical standpoint, the corrosion tests performed with irradiated materials and unirradiated materials are identical except for the additional challenges posed by radiological specimens. However, when the effect of radiation on the corrosive environment (e.g., radiolysis) is the focus, the corrosion test must be performed simultaneously with irradiation, due to the need to capture the dynamic interaction between the ionizing radiation and the corrosive medium. Although radiation-assisted corrosion tests are difficult to perform, they can provide important insights into the unique degradation mechanisms materials may experience in reactor service environments.

5.4. Characterization Methods

Several characterization methods specific to quantifying the features of additively manufactured metals may be employed in addition to the standard techniques for characterizing corrosion. Quantification of surface roughness is needed if as-fabricated surfaces are to be tested; a variety of contact and non-contact profilometry techniques may be employed. Because porosity is a common AM feature affecting almost all properties of additively manufactured materials, it can often be characterized thoroughly via various techniques. Metallurgical methods such as optical and electron microscopy, density measurement, or x-ray tomography may be used to characterize porosity in additively manufactured materials [72]. Basic metallographic techniques can be used to characterize an additively manufactured material's anisotropic grain structure, and post-build heat treatments may be applied to minimize the impact of residual stress. Microstructure characterization methods such as transmission electron microscopy and energy dispersive

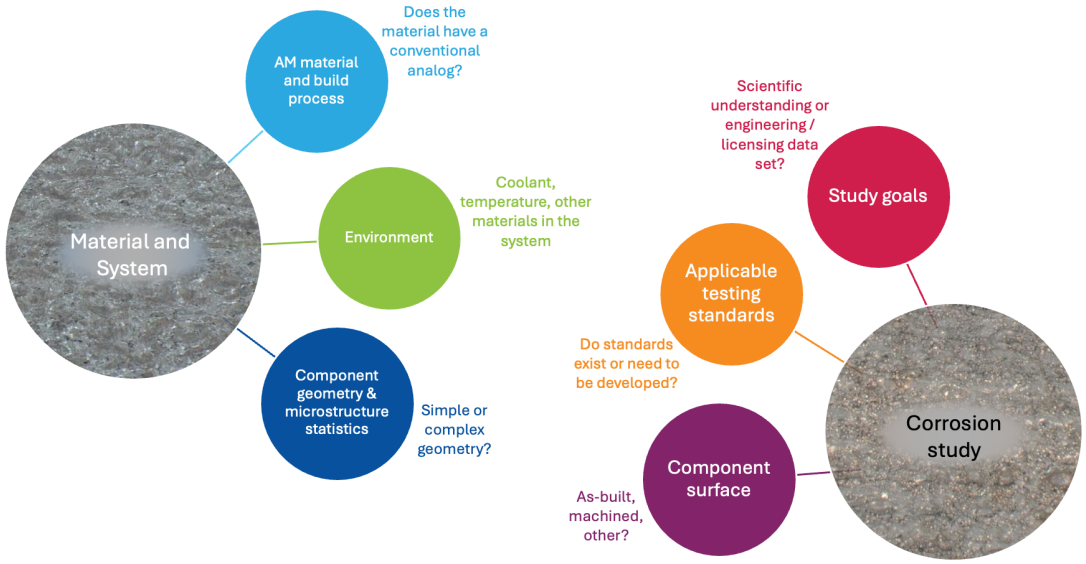

Figure 4: Representation of the conceptual organization that can inform the development of a corrosion test campaign for additively manufactured materials to be deployed in nuclear reactors.

spectroscopy are necessary to acquire detailed information on the inhomogeneous microstructure to analyze its influence on corrosion properties. Aspects of the cellular structure (e.g., dislocation density, cell size, and microsegregation) should be measured.

6. Structuring Corrosion Tests of Additively Manufactured Materials for Nuclear Reactor Applications

A corrosion testing strategy for AM materials must be application-specific given the complexity of AM materials and reactor environments. The decision-making process must center around the additively manufactured material's characteristics that influence the result of the engineering-scale or mesoscale investigations: unique surface finish, compositional and crystallographic inhomogeneities, and residual stresses. A schematic of the suggested decision-making process is presented in Fig. 4.

Given the features of additively manufactured materials (surface roughness, solute segregation, complex microstructure, and residual stresses), some amount of post-build processing generally occurs. The surface may be machined, as previously discussed. Post-build heat treatment is also common for stress relief, solution annealing, or microstructure homogenization [7]. Furthermore, a material may be processed to optimize its structure in light of one particular property (e.g., creep strength), potentially impacting its corrosion behavior. As a result, the corrosion behavior should be assessed for each instantiation of the AM-built and post-processed material in order to reveal how microstructure tuning for a given property and component performance will affect the corrosion behavior.

Corrosion testing can focus on characterizing phenomena of engineering interest (e.g., weight loss/gain, pit and crevice formation, and post-corrosion mechanical response), as well as on understanding corrosion mechanisms at the mesoscale (e.g., the characterization of phases induced by corrosion and local chemistry changes). The specific corrosion testing strategy employed to assess an additively manufactured material for a reactor environment will depend on the degree of prior knowledge pertaining to the behavior of the material composition in that environment. For example, if prior information exists on conventionally manufactured 316H SS in FLiNaK [104], the corrosion testing strategy can leverage this prior knowledge to rank specific corrosion tests by their importance in regard to the material. In such case, a mass transfer test in a flowing salt loop would be a high-priority test. If, however, little or no such information exists, a rapid assessment

campaign of static coupon tests may help gain a sense of how the material performs, such that additional specific tests can then be selected. If a material-environment system is chemically complex and not well understood (e.g., corrosion in molten chloride systems), determination of corrosion species is needed to identify the surface sites most vulnerable to specific species attack, as well as to establish which grain, chemical composition, and microstructure may provide the best corrosion resistance.

Some evidence indicates that, due to surface roughness, as-fabricated, net-shape additively manufactured 316 SS components may have improved corrosion behavior over wrought 316 SS [67]; however, other evidence suggests that rough surfaces increase crevice corrosion [73]. Because additively manufactured components may be deployed without further surface finishing, understanding the effect of the surface texture on corrosion behavior is crucial. Weight measurements, as well as a determination of microstructure and microchemical evolution at the surface, are needed. The presence of porosity and residual stresses is also a concern, as is the formation of oxide phases or atypical inclusions. Given the likelihood of crevice corrosion at the as-built surface, 3D non-destructive examination both before and after corrosion testing is recommended, such as via x-ray computed tomography, which will enable characterization of comparative pre- and post-corrosion porosity at the surface and within the same sample. Upon identifying areas of interest, these specimens can then be sectioned to study microstructure and local composition variation via scanning electron microscopy and transmission electron microscopy imaging.

To understand the effect of surface finishing on the corrosion performance of AM materials, a "two-surface" test with both as-printed and machined coupons can help determine macroscopic and microscopic corrosion behaviors and their underlying mechanisms. As-printed surfaces provide the necessary engineering baseline, while additively manufactured specimens with machined-smooth surfaces can be used to assess the underlying corrosion mechanisms and determine how corrosion is localized to or affected by a rough surface. Wrought specimens can be added to further determine how the AM build process and microstructure affect corrosion. This is especially important if AM processing is being proposed for replacing conventional fabrication of a material currently in service. Similarly, the effect of post-build heat treatments can also be assessed via the two-surface test. In fact, the two-surface test strategy is applicable to a variety of tests such as static corrosion tests, flow tests, and SCC studies.

Process variability should be addressed through a combination of experiments and data analytics. Variability should be considered at both the microscale and macroscale. At the microscale, the statistical distribution of a corrosion behavior of interest should be understood with respect to key microstructural features. Successful assessment of the impact of process variability on corrosion behavior requires data traceability linking sources of process variability (e.g., build parameters, feedstock properties) and microstructure statistics (grain geometries, dislocation cell characteristics, solute distribution) to the corrosion test results. Conversely, macroscale variability can be tested by taking samples from different locations within a given component. The surface finish on a single component can vary depending on the orientation of the surface with respect to the build direction [105]. In general, the inherent process variability (leading to microstructure variability) should be studied, tested, and characterized to determine how impactful it is on corrosion behavior and to place bounds on accepted variability.

In general, corrosion testing of irradiated material is more experimentally challenging. Thus, testing of unirradiated specimens outside a neutron-irradiation environment is recommended as the first step in testing additively manufactured components for deployment in neutron-exposed reactor environments. This is because of the cost and time involved in testing irradiated materials or performing *in situ* irradiation testing. Laboratory testing of unirradiated specimens can answer questions regarding the impact of process variability, post-build treatment, surface finish, and corrosion mechanisms. The second stage of corrosion testing for reactor environments can entail laboratory testing of irradiated additively manufactured materials to determine the impact of irradiation-driven microstructural changes on corrosion behavior. Such changes may be the major driver of irradiation effects on corrosion behavior when the service temperature is elevated sufficiently for rapid defect migration, as in the case of many advanced reactor designs. At lower temperatures, defect production rates may be important. Finally, *in situ* corrosion testing in a reactor may be possible (depending on the availability of test capabilities or surveillance specimens in as-built reactors) for fully prototypical testing, which can account for environmental conditions such as irradiation-induced chemistry changes in the coolant and actual coolant flow rates.

7. Conclusions

AM technologies have developed rapidly in recent years, creating new opportunities and challenges for the nuclear industry. Corrosion-induced degradation and failure are major engineering concerns for nuclear power plants. To adopt AM technologies into nuclear applications, the corrosion performance of additively manufactured materials must be appropriately evaluated. Accordingly, a large array of regulations surrounds corrosion testing and in-reactor assessment. Regulatory bodies for nuclear power plants (e.g., the NRC) include corrosion-induced degradation among their various considerations pertaining to safe reactor operation. To measure corrosion behaviors, a large body of ASTM standards discusses testing methodologies for many different kinds of corrosion and materials. Before any corrosion tests are performed to evaluate a new additively manufactured material, component, or printing process, relevant ASTM standards should be identified. However, not all corrosion tests envisionable for advanced reactor material-environment systems have ASTM standards. In addition, no ASTM standard exists that is specific to the testing of additively manufactured materials. If a relevant standard does not exist, a standardized methodology for this test case should be developed and tested.

Reactor-specific corrosion testing is necessary because of all the different material-environment interactions possible, especially with differences in temperature and coolant type (molten salts, liquid metals, high-temperature gas, and water). In addition, additively manufactured materials and components possess unique characteristics generally not found in wrought materials to the same extent or in the same combinations, including dislocation cell structures, microsegregation at dislocation cells and melt pool boundaries, anisotropic microstructures, unusual phases and inclusions, and appreciable porosity. These features can impact the corrosion behavior of the material. The specific corrosion testing strategy employed for a given reactor environment will depend on the degree of prior knowledge pertaining to the behavior of the material composition in that environment.

In addition, additively manufactured components may be deployed with as-fabricated surfaces, without being machined smooth. This represents a paradigm shift in corrosion testing for nuclear materials, which has generally tested machined specimens. The relation of the specimen surface to the build direction also impacts the resulting surface roughness, adding another variable. The process variability inherent in AM (and which leads to microstructure and surface variability) must be managed via a strategy to determine how impactful this variability is on the corrosion behavior, as well as what the acceptable bounds on the variability are. A two-surface test is proposed that employs as-printed and machined-smooth coupons to determine how AM-specific microstructural features and rough surfaces impact corrosion. Given the likelihood of crevice corrosion on the as-built surface, 3D non-destructive examination both before and after corrosion testing is recommended, such as x-ray computed tomography. For corrosion phenomena involving radiation and irradiated microstructure, a staged approach to testing AM specimens in representative environments is also proposed. Testing unirradiated specimens in a laboratory environment is recommended as the first step. The second stage of corrosion testing for reactor environments should entail *ex situ* testing of irradiated AM material to determine the impact of irradiation-driven microstructural changes on corrosion behavior. Finally, depending on the availability of testing capabilities, *in situ* corrosion testing can follow, exploring possible transient effects induced by irradiation, coolant flow, or temperature gradients.

Acknowledgements

This work was sponsored by the U.S. Department of Energy, Office of Nuclear Energy, Advanced Materials and Manufacturing Technologies program. This manuscript was authored in part by Idaho National Laboratory, which is operated by Battelle Energy Alliance LLC, under contract no. DE-AC07-05ID14517; by Argonne National Laboratory, which is managed and operated by UChicago Argonne LLC, under contract no. DE-AC02-06CH11357, and by Pacific Northwest National Laboratory, which is operated by Battelle Memorial Institute, under contract no. DE-AC05-76RL01830.

References

[1] W. J. Sames, F. List, S. Pannala, R. R. Dehoff, S. S. Babu, The metallurgy and processing science of metal additive manufacturing, International Materials Reviews 61 (5) (2016) 315–360.

[2] Advanced Reactor Roadmap Phase 1: North America, Tech. Rep. 3002027504, Electric Power Research Institute and Nuclear Energy Institute, Palo Alto, California (May 2023).

[3] G. Sander, J. Tan, P. Balan, O. Gharbi, D. R. Feenstra, L. Singer, S. Thomas, R. G. Kelly, J. R. Scully, N. Birbilis, Corrosion of additively manufactured alloys: A review, Corrosion 74 (12) (2018) 1318.

[4] M. Li, D. Andersson, R. Dehoff, A. Jokisaari, I. V. Rooyen, D. Cairns-Gallimore, Advanced Materials and Manufacturing Technologies (AMMT) 2022 Roadmap, Tech. Rep. ANL-23/12, Argonne National Laboratory (September 2022).

[5] A. Vafadar, F. Guzzomi, A. Rassau, K. Hayward, Advances in metal additive manufacturing: A review of common processes, industrial applications, and current challenges, Applied Sciences 11 (2021) 1213.

[6] G. Liu, X. Zhang, X. Chen, Y. He, L. Cheng, M. Huo, H. Yin, F. Hao, S. Chen, P. Wang, S. Yi, L. Wan, Z. Mao, Z. Chen, X. Wang, Z. Cao, J. Lu, Additive manufacturing of structural materials, Materials Science & Engineering R 145 (2021) 100596.

[7] T. Wohlers, I. Campbell, O. Diegel, R. Huff, J. Kowen, 3D printing and additive manufacturing state of the industry, Tech. rep., Lund University, Lund, Sweden (2017).

[8] R. Russell, D. Wells, J. Waller, B. Poorganji, E. Ott, T. Nakagawa, H. Sandoval, N. Shamsaei, M. Seifi, Qualification and certification of metal additive manufactured hardware for aerospace applications, in: Additive Manufacturing for the Aerospace Industry, Elsevier, Amsterdam, The Netherlands, 2019.

[9] Nuclear Energy Institute, Roadmap for regulatory acceptance of advanced manufacturing methods in the nuclear energy industry, May 13, 2019 (2019).

[10] R. B. Rebak, X. Lou, Environmental cracking and irradiation resistant stainless steels by additive manufacturing, Technical Report NE0008428, GE Global Research (March 2018).

[11] D. W. Gandy, Strategy and approach for qualification of nuclear components produced via additive manufacturing, in: US DOE Advanced Methods of Manufacturing Workshop, US Department of Energy, Germantown, MD, USA, 2016.

[12] U.S. Nuclear Regulatory Commission, Action plan for advanced manufacturing technologies, Revision 1, Tech. Rep. ML19333B980, U.S. Nuclear Regulatory Commission, Washington, DC (2020).

[13] J. Simpson, J. Haley, C. Cramer, O. Shafer, A. Elliott, W. Peter, L. Love, R. Dehoff, Considerations for application of additive manufacturing to nuclear reactor core components, Tech. rep., ORNL/TM-2019/1190, M3CT-19OR06090123 (2019).

[14] Corrosion costs and preventative strategies in the United States, Tech. rep., NACE International, Houston, Texas (2016).

[15] X. Zhang, F. Liou, Chapter 1: Introduction to additive manufacturing, in: J. Pou, A. Riveriro, J. P. Davim (Eds.), Handbooks in Advanced Manufacturing-Additive Manufacturing, Elsevier Inc, 2021, pp. 1–31.

[16] M. D. Shamsujjoha, S. R. Agnew, J. M. Fitzgerald, W. R. Moore, T. A. Newman, High strength and ductility of additively manufactured 316L stainless steel explained, Metallurgical and Materials Transactions A 49 (A) (2018) 3011.

[17] M. Li, X. Zhang, W.-Y. Chen, T. S. Byun, Creep behavior of 316L stainless steel manufactured by laser powder bed fusion, Journal of Nuclear Materials 548 (2021) 152847.

[18] D. A. Jones, Princles and prevention of corrosion, Second edition, Prentice Hall, Upper Saddle River, NJ, 1996.

[19] G. S. Was, Fundamentals of Radiation Materials Science, Springer New York, New York, NY, 2017.

[20] P. Crook, D. Klarstrom, J. Crum, Corrosion of nickel and nickel-base alloys, in: S. D. Cramer, B. S. Covino Jr. (Eds.), ASM Handbook Volume 13B Corrosion: Materials, ASM International, Materials Park, OH, 2005, pp. 228–231.

[21] J. F. Grubb, T. DeBold, J. D. Fritz, Corrosion of wrought stainless steels, in: S. D. Cramer, B. S. Covino Jr. (Eds.), ASM Handbook Volume 13B Corrosion: Materials, ASM International, Materials Park, OH, 2005, pp. 54–75.

[22] V. Ĉíhal, I. Kašová, Relation between carbide precipitation and intercrystalline corrosion of stainless steels, Corrosion science 10 (12) (1970) 875–881.

[23] P. Breeze, Chapter 17 - nuclear power, in: P. Breeze (Ed.), Power Generation Technologies (Third Edition), third edition Edition, Newnes, 2019, pp. 399–429. doi:https://doi.org/10.1016/B978-0-08-102631-1.00017-1.
URL https://www.sciencedirect.com/science/article/pii/B9780081026311000171

[24] A. T. Motta, A. Couet, R. J. Comstock, Corrosion of zirconium alloys used for nuclear fuel cladding, Annual Review of Materials Research 45 (2015) 311–343.

[25] F. P. Ford, P. L. Andresen, Corrosion in nuclear systems: environmentally assisted cracking in light water reactors, P. Marcus and J. Ouder, Marcel Dekker (1994) 501–546.

[26] J. T. Busby, Overview of structural materials in water-cooled fission reactors, in: Structural alloys for nuclear energy applications, Elsevier, 2019, pp. 1–22.

[27] W. J. Shack, T. F. Kassner, P. S. Maiya, J. Y. Park, W. E. Ruther, BWR pipe crack and weld overlay studies, Nuclear Engineering and Design 89 (2-3) (1985) 295.

[28] F. Ford, P. Andresen, Development and use of a predictive model of crack propagation in 304/316L, A533B/A508 and Inconel 600/182 alloys in 288 C water, in: Proceedings of the third international symposium on environmental degradation of materials in nuclear power systems, 1988.

[29] B. Arsenault, E. Ghali, Stress corrosion cracking of pressure vessel welded carbon steels, International Journal of Pressure Vessels and Piping 45 (1) (1991) 23–41.

[30] G. S. Was, Recent developments in understanding irradiation assisted stress corrsion cracking, in: Proceedings of the 11th International Conference on Environmental Degradation of Materials in Nuclear Power Systems-Water Reactors, Stevenson, Washington, Aug. 10-14, 2003, Am. Nucl. Soc., 2003.

[31] A. Hirano, K. Sakaguchi, T. Shoji, Effects of water flow rate on fatigue life of structural steels under simulated BWR environment, in: ASME Pressure Vessels and Piping Conference, Vol. 42797, 2007, pp. 231–242.

[32] K. Sridharan, T. Allen, Corrosion in molten salts, in: F. Lantelme, H. Groult (Eds.), Molten salts chemistry, Elsevier, 2013, pp. 241–267.

[33] S. S. Raiman, S. Lee, Aggregation and data analysis of corrosion studies in molten chloride and fluoride salts, Journal of Nuclear Materials 511 (2018) 523–535.

[34] J. Zhang, C. W. Forsberg, M. F. Simpson, S. Guo, S. T. Lam, R. O. Scarlat, F. Carotti, K. J. Chan, P. M. Singh, W. Doniger, et al., Redox potential control in molten salt systems for corrosion mitigation, Corrosion Science 144 (2018) 44–53.

[35] M. Ho, G. Yeoh, G. Braoudakis, Molten salt reactors, Materials and Processes for Energy, Formatex (2013) 761–768.

[36] S. Guo, J. Zhang, W. Wu, W. Zhou, Corrosion in the molten fluoride and chloride salts and materials development for nuclear applications, Progress in Materials Science 97 (2018) 448–487.

[37] J. Koger, Corrosion product deposition in molten fluoride salt systems, Corrosion 30 (4) (1974) 125–130.

[38] K. Aoto, P. Dufour, Y. Hongyi, J. P. Glatz, Y.-i. Kim, Y. Ashurko, R. Hill, N. Uto, A summary of sodium-cooled fast reactor development, Progress in Nuclear Energy 77 (2014) 247–265.

[39] G. S. Was, T. R. Allen, Corrosion issues in current and next-generation nuclear reactors, Structural Alloys for Nuclear Energy Applications (2019) 211–246.

[40] M. Li, K. Natesan, W.-Y. Chen, Material performance in sodium, in: Comprehensive Nuclear Materials 2nd Edition, Vol. 4, Elsevier, Oxford, 2020, pp. 339–356.

[41] V. Ganesan, V. Ganesan, H. Borgstedt, Analysis of crevona sodium loop material, Journal of nuclear materials 312 (2-3) (2003) 174–180.

[42] E. Yoshida, S. Kato, Sodium compatibility of ODS steel at elevated temperature, Journal of Nuclear Materials 329 (2004) 1393–1397.

[43] E. Yoshida, T. Furukawa, Corrosion issues in sodium-cooled fast reactor (SFR) systems, in: Nuclear Corrosion Science and Engineering, Elsevier, 2012, pp. 773–806.

[44] O. Sreedharan, B. Madan, J. Gnanamoorthy, Threshold oxygen levels in Na (l) for the formation of $NaCrO_2$ (s) on 18-8 stainless steels from accurate thermodynamic measurements, Journal of Nuclear Materials 119 (2-3) (1983) 296–300.

[45] M. O. Rothwell, Cold trap performance: a general analysis, Ph.D. thesis, Oregon State University (1972).

[46] D. Sandusky, J. Armijo, W. Wagner, Influence of long-term sodium exposure on the composition and microstructure of austenitic alloys, Journal of Nuclear Materials 46 (3) (1973) 225–243.

[47] T. Allen, D. Crawford, et al., Lead-cooled fast reactor systems and the fuels and materials challenges, Science and Technology of Nuclear Installations 2007 (2007).

[48] C. Schroer, O. Wedemeyer, J. Konys, Aspects of minimizing steel corrosion in liquid lead-alloys by addition of oxygen, in: International Conference on Nuclear Engineering, Vol. 49330, 2010, pp. 207–218.

[49] X. Gong, R. Li, M. Sun, Q. Ren, T. Liu, M. P. Short, Opportunities for the LWR ATF materials development program to contribute to the LBE-cooled ADS materials qualification program, Journal of Nuclear Materials 482 (2016) 218–228.

[50] R. Quade, A. McMain, Hydrogen production with a high-temperature gas-cooled reactor (HTGR), in: Hydrogen Energy: Part A, Springer, 1975, pp. 137–154.

[51] L.-R. Liu, T. Jin, N.-R. Zhao, Z. Wang, X. Sun, H. Guan, Z. Hu, Effect of carbon addition on the creep properties in a ni-based single crystal superalloy, Materials Science and Engineering: A 385 (1-2) (2004) 105–112.

[52] D. Kumar, R. R. Adharapurapu, T. M. Pollock, G. S. Was, High-temperature oxidation of Alloy 617 in helium containing part-per-million levels of CO and CO_2 as impurities, Metallurgical and Materials Transactions A 42 (2011) 1245–1265.

[53] G. S. Was, D. Petti, S. Ukai, S. Zinkle, Materials for future nuclear energy systems, Journal of Nuclear Materials 527 (2019) 151837.

[54] N. D. B. Ezell, S. S. Raiman, J. M. Kurley, J. McDuffee, Neutron irradiation of Alloy N and 316L stainless steel in contact with a molten chloride salt, Nuclear Engineering and Technology 53 (3) (2021) 920–926.

[55] F. Schmidt, P. Hosemann, R. O. Scarlat, D. K. Schreiber, J. R. Scully, B. P. Uberuaga, Effects of radiation-induced defects on corrosion, Annual Review of Materials Research 51 (2021) 293–328.

[56] W. Zhou, Y. Yang, G. Zheng, K. B. Woller, P. W. Stahle, A. M. Minor, M. P. Short, Proton irradiation-decelerated intergranular corrosion of Ni-Cr alloys in molten salt, Nature Communications 11 (1) (2020) 3430.

[57] P. Okamoto, L. Rehn, Radiation-induced segregation in binary and ternary alloys, Journal of Nuclear Materials 83 (1) (1979) 2–23.

[58] J. Stiegler, L. Mansur, Radiation effects in structural materials, Annual Review of Materials Science 9 (1) (1979) 405–454.

[59] P. Scott, A review of irradiation assisted stress corrosion cracking, Journal of Nuclear Materials 211 (2) (1994) 101–122.

[60] N. AlMousa, W. Zhou, K. B. Woller, M. P. Short, Effects of simultaneous proton irradiation on the corrosion of commercial alloys in molten fluoride salt, Corrosion Science 217 (2023) 111154.

[61] R. Kilian, A. Roth, Corrosion behaviour of reactor coolant system materials in nuclear power plants, Materials and Corrosion 53 (10) (2002) 727–739.

[62] MCB Issue List Regarding APR-1400, FSAR Section 5.4.2.1, `https://www.nrc.gov/docs/ML1817/ML18172A314.pdf`.

[63] U.S. Nuclear Regulatory Commission, Material compaitibility for non-light water reactors, interim staff guidance, Tech. Rep. ML23188A178, U.S. Nuclear Regulatory Commission, Washington, DC (2023).

[64] T. DebRoy, H. Wei, J. Zuback, T. Mukherjee, J. Elmer, J. Milewski, A. M. Beese, A. d. Wilson-Heid, A. De, W. Zhang, Additive manufacturing of metallic components–process, structure and properties, Progress in Materials Science 92 (2018) 112–224.

[65] C. Örnek, Additive manufacturing – A general corrosion perspective, Corrosion Engineering, Science and Technology 53 (7) (2018) 531–535.

[66] E. J. Schindelholz, M. A. Melia, J. M. Rodelas, Corrosion of additively manufactured stainless steels—process, structure, performance: A review, Corrosion 77 (5) (2021) 484–503.

[67] T. Voisin, R. Shi, Y. Zhu, Z. Qi, M. Wu, S. Sen-Britain, Y. Zhang, S. Qiu, Y. Wang, S. Thomas, et al., Pitting corrosion in 316L stainless steel fabricated by laser powder bed fusion additive manufacturing: A review and perspective, JOM 74 (4) (2022) 1668–1689.

[68] R. I. Revilla, M. Van Calster, M. Raes, G. Arroud, F. Andreatta, L. Pyl, P. Guillaume, I. De Graeve, Microstructure and corrosion behavior of 316L stainless steel prepared using different additive manufacturing methods: A comparative study bringing insights into the impact of microstructure on their passivity, Corrosion Science 176 (2020) 108914.

[69] X. Lou, M. Song, P. W. Emigh, M. A. Othon, P. L. Andresen, On the stress corrosion crack growth behavior in high temperature water of 316L stainless steel made by laser powder bed fusion additive manufacturing, Corrosion Science 128 (2017) 140–153.

[70] M. A. Melia, H.-D. A. Nguyen, J. M. Rodelas, E. J. Schindelholz, Corrosion properties of 304L stainless steel made by directed energy deposition additive manufacturing, Corrosion Science 152 (2019) 20–30.

[71] D. Kong, C. Dong, X. Ni, L. Zhang, H. Luo, R. Li, L. Wang, C. Man, X. Li, Superior resistance to hydrogen damage for selective laser melted 316L stainless steel in a proton exchange membrane fuel cell environment, Corrosion Science 166 (2020) 108425.

[72] C. Man, C. Dong, T. Liu, D. Kong, D. Wang, X. Li, The enhancement of microstructure on the passive and pitting behaviors of selective laser melting 316L stainless steel in simulated body fluid, Applied Surface Science 467 (2019) 193–205.

[73] R. F. Schaller, A. Mishra, J. M. Rodelas, J. M. Taylor, E. J. Schindelholz, The role of microstructure and surface finish on the corrosion of selective laser melted 304, Journal of the Electrochemical Society 165 (5) (2018) C234.

[74] Y. Nakao, K. Nishimoto, Effects of laser surface melting on steel and nickel-base alloy clad corrosion resistance of stainless layers in cast bimetallic pipes, ISIJ International 33 (9) (1993) 934–940.

[75] J. Bedmar, N. Abu-Warda, S. García-Rodríguez, B. Torres, J. Rams, Influence of the surface state on the corrosion behavior of the 316 L stainless steel manufactured by laser powder bed fusion, Corrosion Science 207 (2022) 110550.

[76] S. Sen-Britain, S. Cho, S. Kang, Z. Qi, S. Khairallah, D. Rosas, V. Som, T. T. Li, S. Roger Qiu, Y. Morris Wang, et al., Critical role of slags in pitting corrosion of additively manufactured stainless steel in simulated seawater, Nature Communications 15 (1) (2024) 867.

[77] J. Yang, L. Hawkins, L. He, S. Mahmood, M. Song, K. Schulze, X. Lou, Intragranular irradiation-assisted stress corrosion cracking (IASCC) of 316L stainless steel made by laser direct energy deposition additive manufacturing: Delta ferrite-dislocation channel interaction, Journal of Nuclear Materials 577 (2023) 154305.

[78] I. Segura, L. Murr, C. Terrazas, D. Bermudez, J. Mireles, V. Injeti, K. Li, B. Yu, R. Misra, R. Wicker, Grain boundary and microstructure engineering of Inconel 690 cladding on stainless-steel 316L using electron-beam powder bed fusion additive manufacturing, Journal of Materials Science & Technology 35 (2) (2019) 351–367.

[79] M. N. Gussev, N. Sridharan, S. Babu, K. A. Terrani, Influence of neutron irradiation on Al-6061 alloy produced via ultrasonic additive manufacturing, Journal of Nuclear Materials 550 (2021) 152939.

[80] N. Haghdadi, M. Laleh, M. Moyle, S. Primig, Additive manufacturing of steels: a review of achievements and challenges, Journal of Materials Science 56 (2021) 64–107.

[81] X. Zhang, X. Zhou, T. Hashimoto, L. Bin, Localized corrosion in AA2024-T351 aluminium alloy: Transition from intergranular corrosion to crystallographic pitting, Materials Characterization 130 (2017) 230–236.

[82] J. L. Bartlett, X. Li, An overview of residual stresses in metal powder bed fusion, Additive Manufacturing 27 (2019) 131–149.

[83] A. Sola, A. Nouri, Microstructural porosity in additive manufacturing: The formation and detection of pores in metal parts fabricated by powder bed fusion, Journal of Advanced Manufacturing and Processing 1 (3) (2019) e10021.

[84] H. L. Wei, J. Mazumder, T. DebRoy, Evolution of solidification texture during additive manufacturing, Scientific Reports 5 (2015) 16446.

[85] B. Alexandreanu, X. Zhang, Y. Chen, W.-Y. Chen, M. Li, Mechanical testing of additively manufactured materials, Tech. Rep. ANL/NSE-22/83, Argonne National Laboratory (2022).

[86] G. Sander, S. Thomas, V. Cruz, M. Jurg, N. Birbilis, X. Gao, M. Brameld, C. Hutchinson, On the corrosion and metastable pitting characteristics of 316L stainless steel produced by selective laser melting, Journal of the electrochemical society 164 (6) (2017) C250.

[87] C. Wang, P. Zhu, F. Wang, Y. Lu, T. Shoji, Anisotropy of microstructure and corrosion resistance of 316L stainless steel fabricated by wire and arc additive manufacturing, Corrosion Science 206 (2022) 110549.

[88] X. Chen, J. Li, X. Cheng, H. Wang, Z. Huang, Effect of heat treatment on microstructure, mechanical and corrosion properties of austenitic stainless steel 316L using arc additive manufacturing, Materials Science and Engineering: A 715 (2018) 307–314.

[89] G. Ko, W. Kim, K. Kwon, T.-K. Lee, The corrosion of stainless steel made by additive manufacturing: A review, Metals 11 (3) (2021) 516.

[90] P. Deng, M. Karadge, R. B. Rebak, V. K. Gupta, B. C. Prorok, X. Lou, The origin and formation of oxygen inclusions in austenitic stainless steels manufactured by laser powder bed fusion, Additive Manufacturing 35 (2020) 101334.

[91] P. Deng, M. Song, J. Yang, Q. Pan, S. McAllister, L. Li, B. C. Prorok, X. Lou, On the thermal coarsening and transformation of nanoscale oxide inclusions in 316l stainless steel manufactured by laser powder bed fusion and its influence on impact toughness, Materials Science and Engineering: A 835 (2022) 142690.

[92] X. Lou, P. L. Andresen, R. B. Rebak, Oxide inclusions in laser additive manufactured stainless steel and their effects on impact toughness and stress corrosion cracking behavior, Journal of Nuclear Materials 499 (2018) 182–190.

[93] J. H. Park, Y. Kang, Inclusions in stainless steels- a review, steel research international 88 (12) (2017) 1700130.

[94] K. Bertsch, G. M. De Bellefon, B. Kuehl, D. Thoma, Origin of dislocation structures in an additively manufactured austenitic stainless steel 316l, Acta Materialia 199 (2020) 19–33.

[95] D. J. Sprouster, W. S. Cunningham, G. P. Halada, H. Yan, A. Pattammattel, X. Huang, D. Olds, M. Tilton, Y. S. Chu, E. Dooryhee, et al., Dislocation microstructure and its influence on corrosion behavior in laser additively manufactured 316L stainless steel, Additive Manufacturing 47 (2021) 102263.

[96] L. Nuñez, C. M. Downey, I. J. van Rooyen, I. Charit, M. R. Maughan, Analysis of surface roughness in metal directed energy deposition, The International Journal of Advanced Manufacturing Technology (2024) 1–20.

[97] K. Li, W. Chen, N. Gong, H. Pu, J. Luo, D. Z. Zhang, L. E. Murr, A critical review on wire-arc directed energy deposition of high-performance steels, Journal of Materials Research and Technology (2023).

[98] D. Obilanade, C. Dordlofva, P. Törlind, Surface roughness considerations in design for additive manufacturing-a literature review, Proceedings of the design society 1 (2021) 2841–2850.

[99] K. Jahns, R. Bappert, P. Böhlke, U. Krupp, Additive manufacturing of cucr1zr by development of a gas atomization and laser powder bed fusion routine, The International Journal of Advanced Manufacturing Technology 107 (5) (2020) 2151–2161.

[100] Creative commons attribution 4.0 international license, `https://creativecommons.org/licenses/by/4.0/`, accessed: 2024-04-30.

[101] J. Ge, J. Lin, Y. Chen, Y. Lei, H. Fu, Characterization of wire arc additive manufacturing 2cr13 part: Process stability, microstructural evolution, and tensile properties, Journal of Alloys and Compounds 748 (2018) 911–921.

[102] R. J. Hebert, Metallurgical aspects of powder bed metal additive manufacturing, Journal of Materials Science 51 (2016) 1165–1175.

[103] J. R. Davis, Corrosion: Understanding the Basics, ASM International, 2000.

[104] S. S. Raiman, J. M. Kurley, D. Sulejmanovic, A. Willoughby, S. Nelson, K. Mao, C. M. Parish, M. S. Greenwood, B. A. Pint, Corrosion of 316H stainless steel in flowing FLiNaK salt, Journal of Nuclear Materials 561 (2022) 153551.

[105] F. Cabanettes, A. Joubert, G. Chardon, V. Dumas, J. Rech, C. Grosjean, Z. Dimkovski, Topography of as built surfaces generated in metal additive manufacturing: A multi scale analysis from form to roughness, Precision Engineering 52 (2018) 249–265.